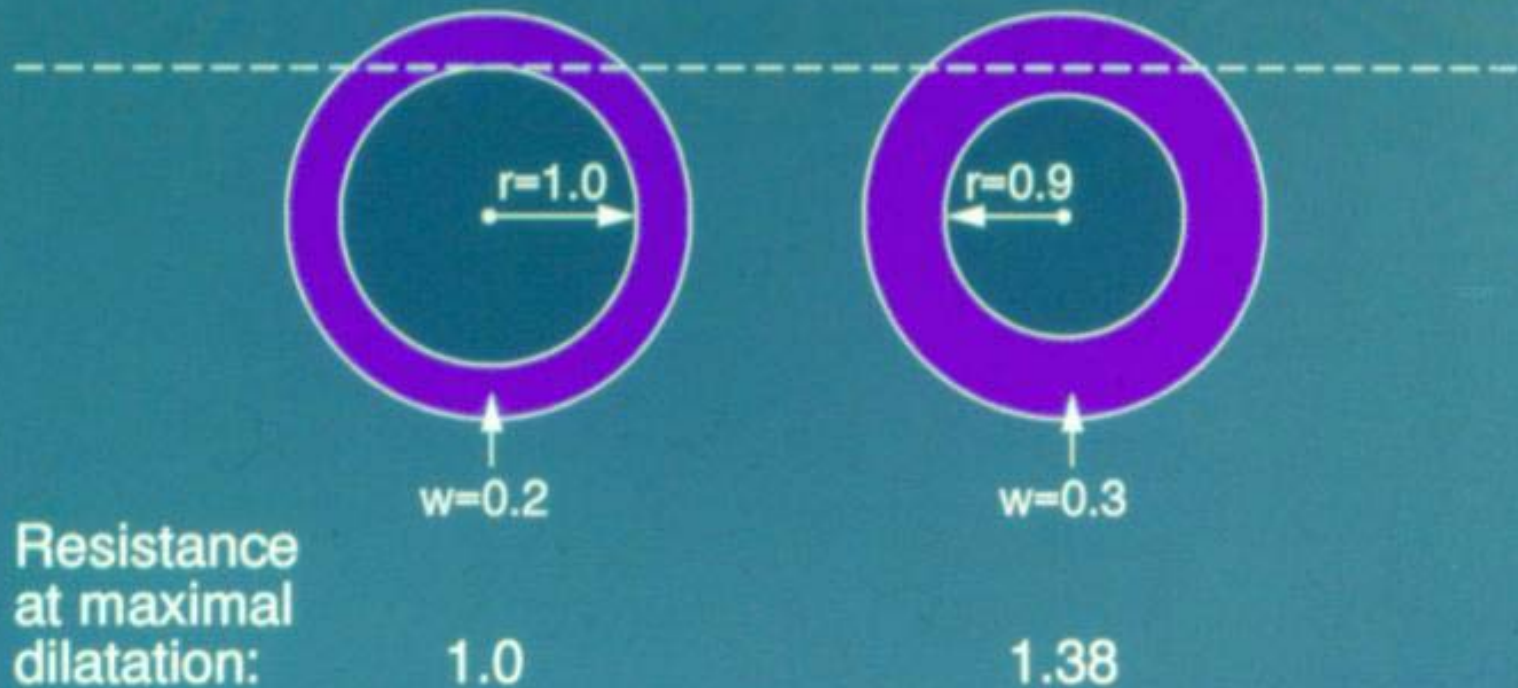


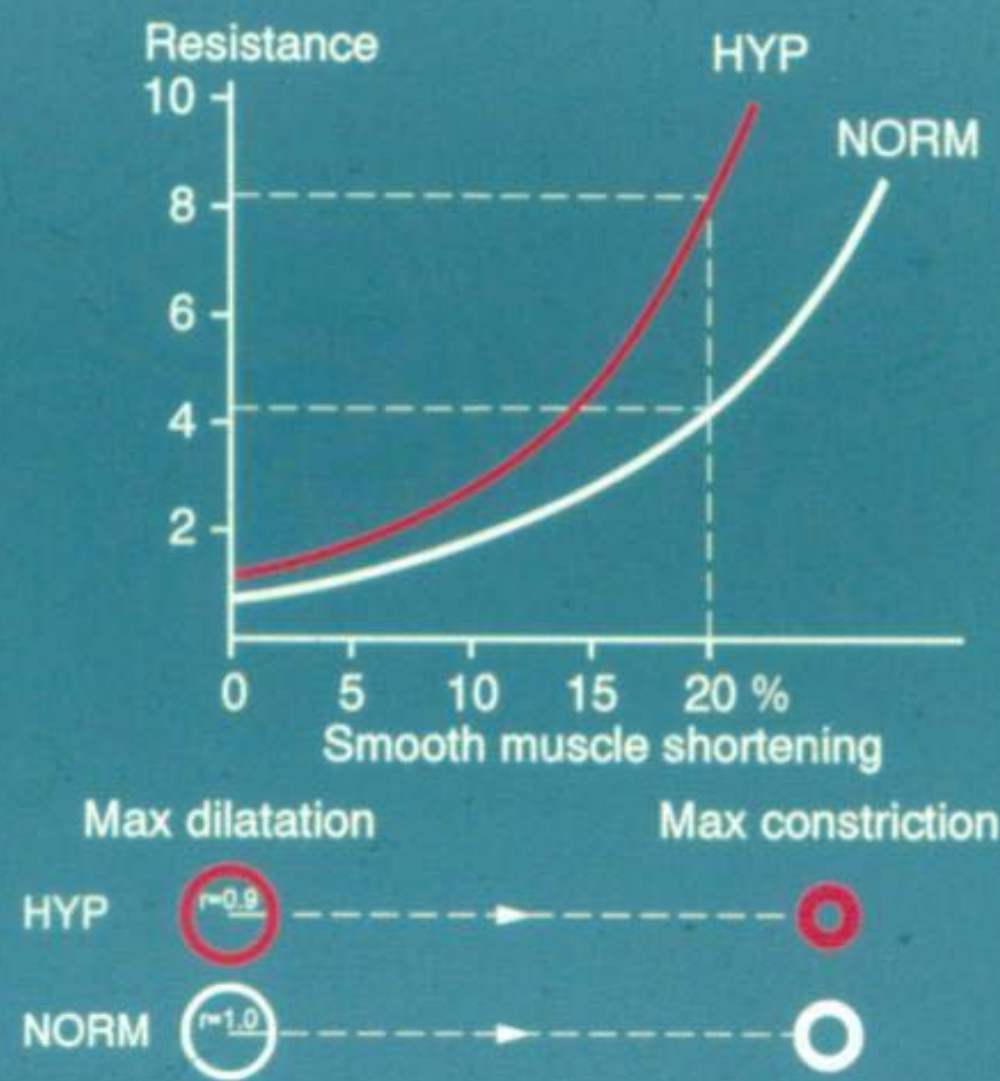
# Structural autoregulation

Normotension

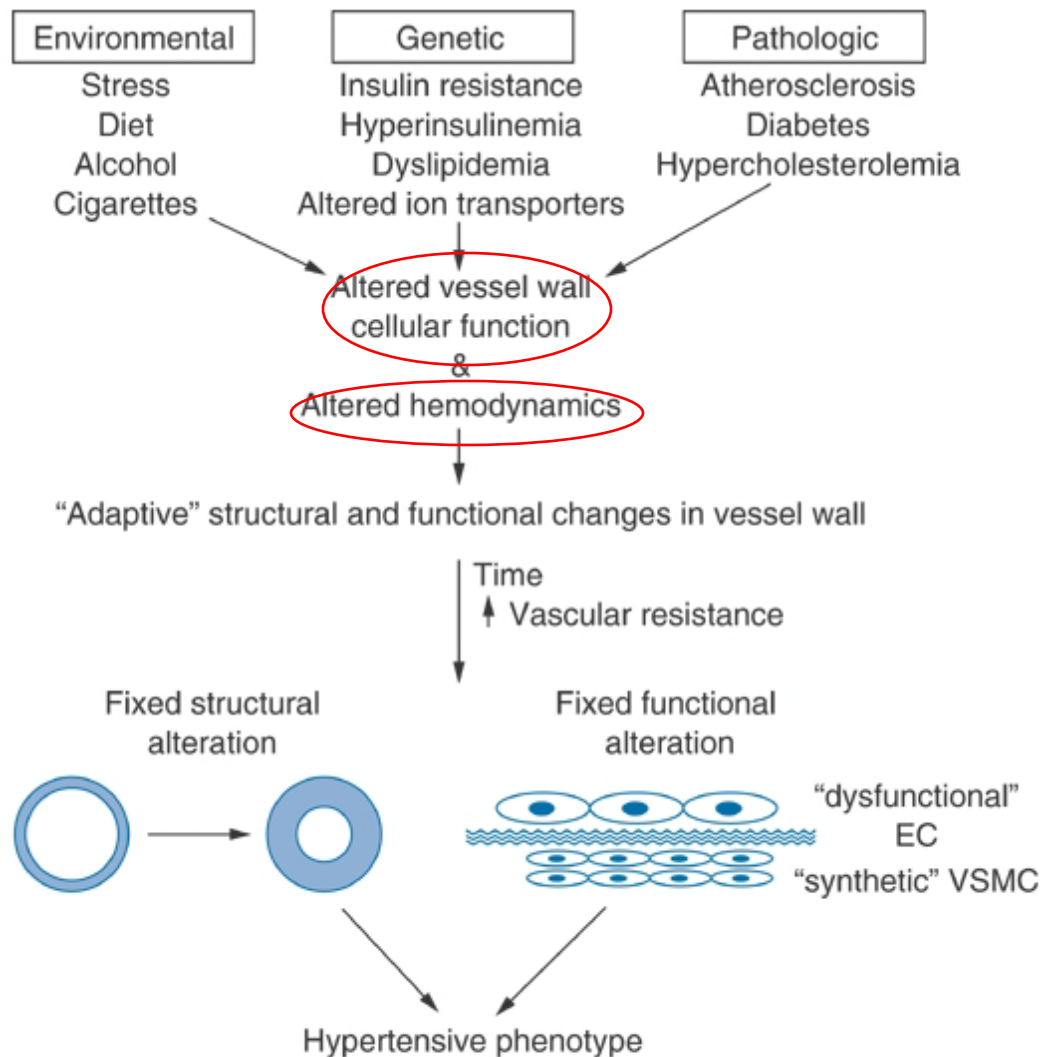
Hypertension



# Resistance vessel hypertrophy increases peripheral resistance



(Folkow et al 1958)

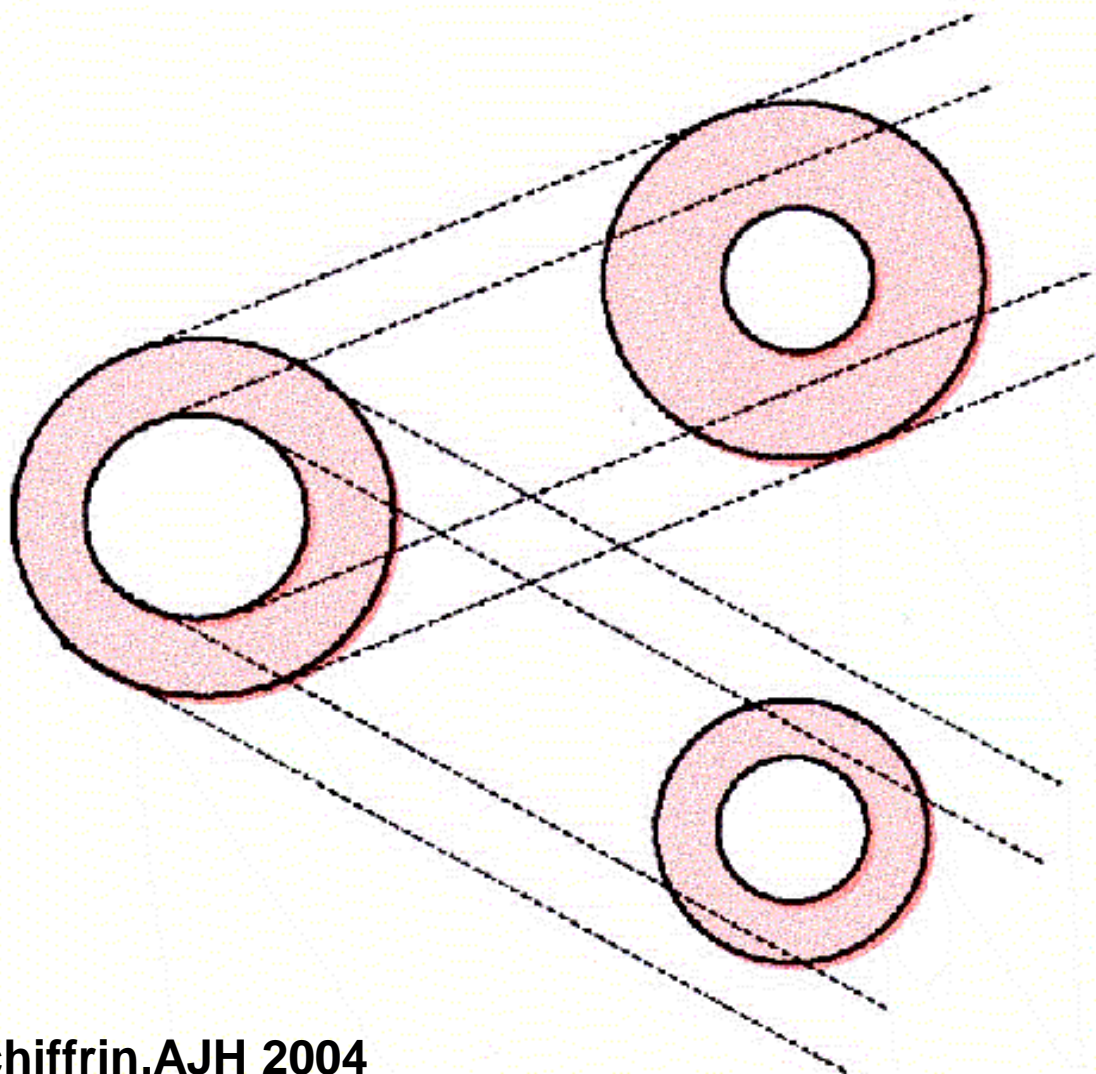


Model for development of structural and functional alterations characteristic of the hypertensive vessel wall. EC, endothelial cell; VSMC, vascular smooth muscle cell.



**Normotensive**

**Hypertensive**

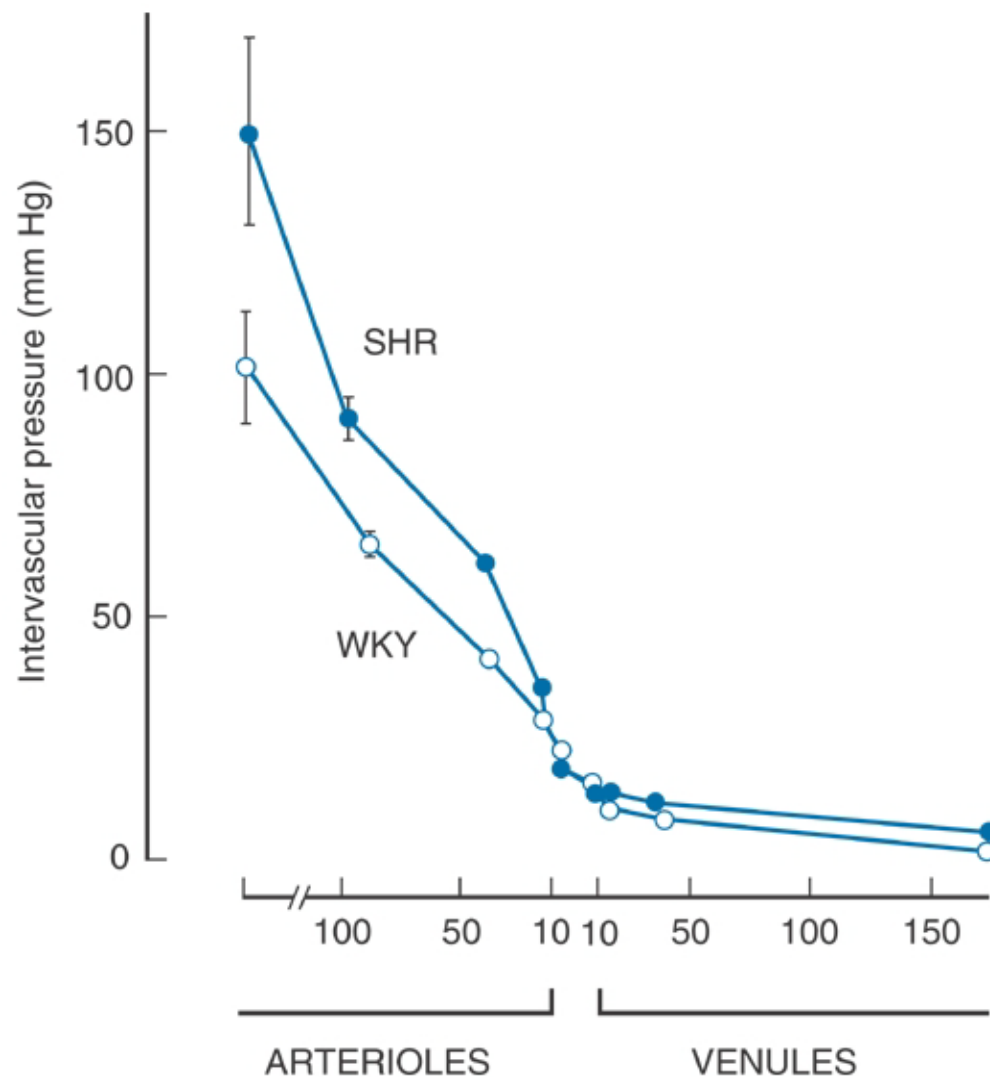


**Hypertrophic  
Remodeling**  
↑ Media/lumen  
↑ CSA  
(endothelin)

**Eutrophic  
Remodeling**  
↑ Media/lumen  
= CSA  
(angiotensin II)

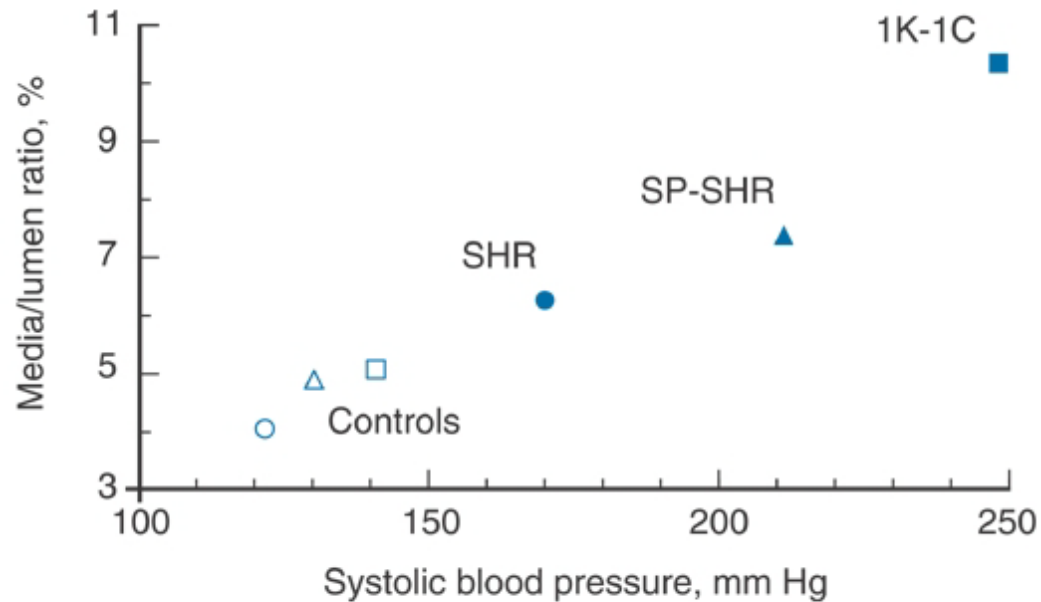






Pressure profile in the vasculature of the spontaneously hypertensive rat (SHR) and the normotensive Wistar-Kyoto (WKY) rat. The relationship between intravascular pressure and vessel diameter (in micrometers) shows a significantly greater pressure at any diameter in the SHR.

(Modified from Mulvany MJ: Vascular structure and smooth muscle contractility in experimental hypertension. *J Cardiovasc Pharmacol* 6[suppl]:S79, 1987.)



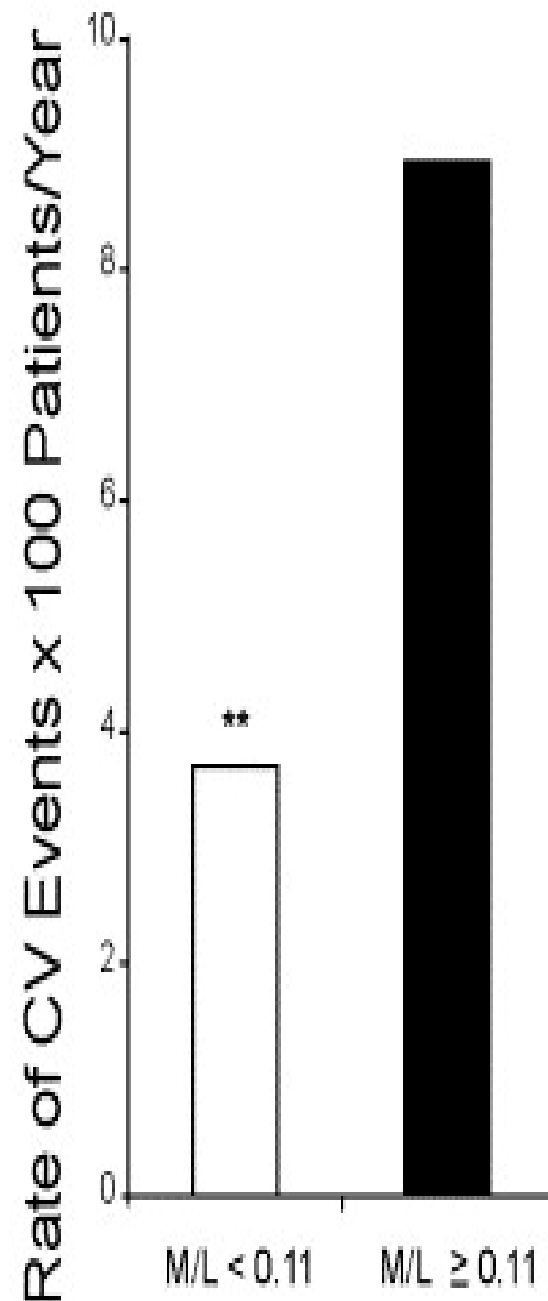
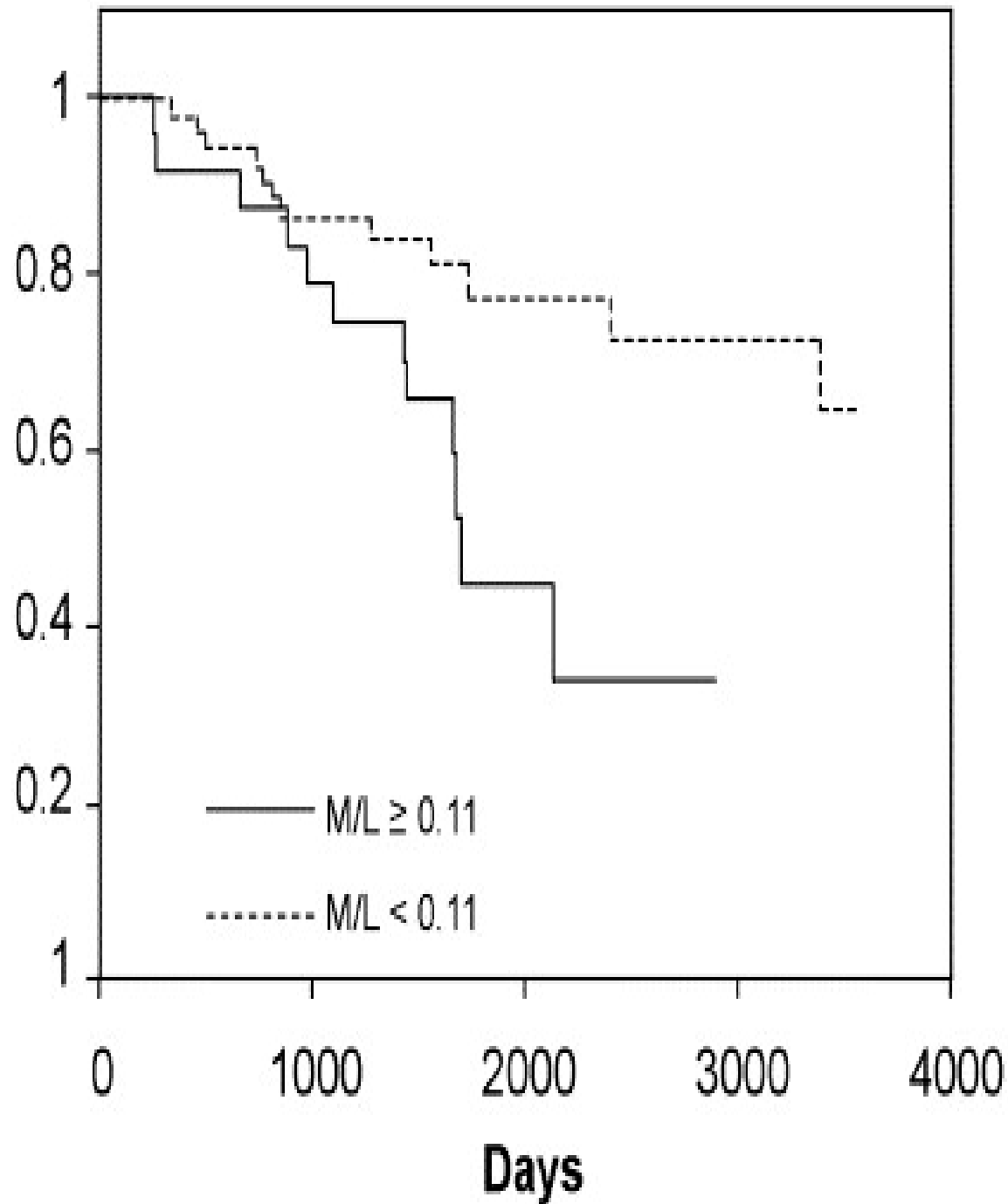
The media/lumen ratio correlates with the systolic blood pressure in hypertensive rats. Both genetic models of hypertension (spontaneously hypertensive rats [SHR], stroke-prone [SP-SHR]) and induced models (one-kidney one-clip [1K-1C]) show a positive correlation between the blood pressure and the percentage of the media relative to the lumen.

(Modified from Mulvany MJ: Vascular structure and smooth muscle contractility in experimental hypertension. J Cardiovasc Pharmacol 6[suppl]:S79, 1987.)

© 2004, 2000, 1996, 1991, 1986, 1981, 1976, Elsevier Inc. All rights reserved.



Event-Free Survival



Rizzoni et al, Circ 2003

# Smooth Muscle Cell Growth Factors in Essential Hypertension

GROWTH FACTOR	CELL SOURCE	REGULATED BY
Angiotensin II	SMC	ACE Angiotensinogen Renin
Endothelin	EC	<u>TGF-<math>\beta</math></u> , Trombin, <u>Angiotensin</u> , arginine <u>Vasopressin</u> , <u>shear stress</u> , <u>PDGF AA</u>
Vasopressin	Nerves	Autonomic activity
Epidermal growth factor (EGF)	Platelets Salivary gland	Unknown, ? Testosterone
Fibroblast growth factor (FGF)	EC SMC	Unknown

Berk, Brenner-Rector 2004

# Smooth Muscle Cell Growth Factors in Essential Hypertension

GROWTH FACTOR	CELL SOURCE	REGULATED BY
Trombin	Liver	EC prothrombotic state
Insulin-like growth factor (IGF)	SMC	<u>Angiotensin II</u> Stimulated by <u>PDGF</u> and <u>Epi dermal growth factor</u> ↑ Shear Stress
Platelet derived growth Factor (PDGF)	EC SMC	<u>Angiotensin II</u>
Transforming Growth factor (TGF- $\beta$ )	SMC Platelets	<u>Angiotensin II</u>
Norepinephrine and catecholamines	Nerves	Central nervous system
Serotonin	Platelets Nerves	EC prothrombotic state

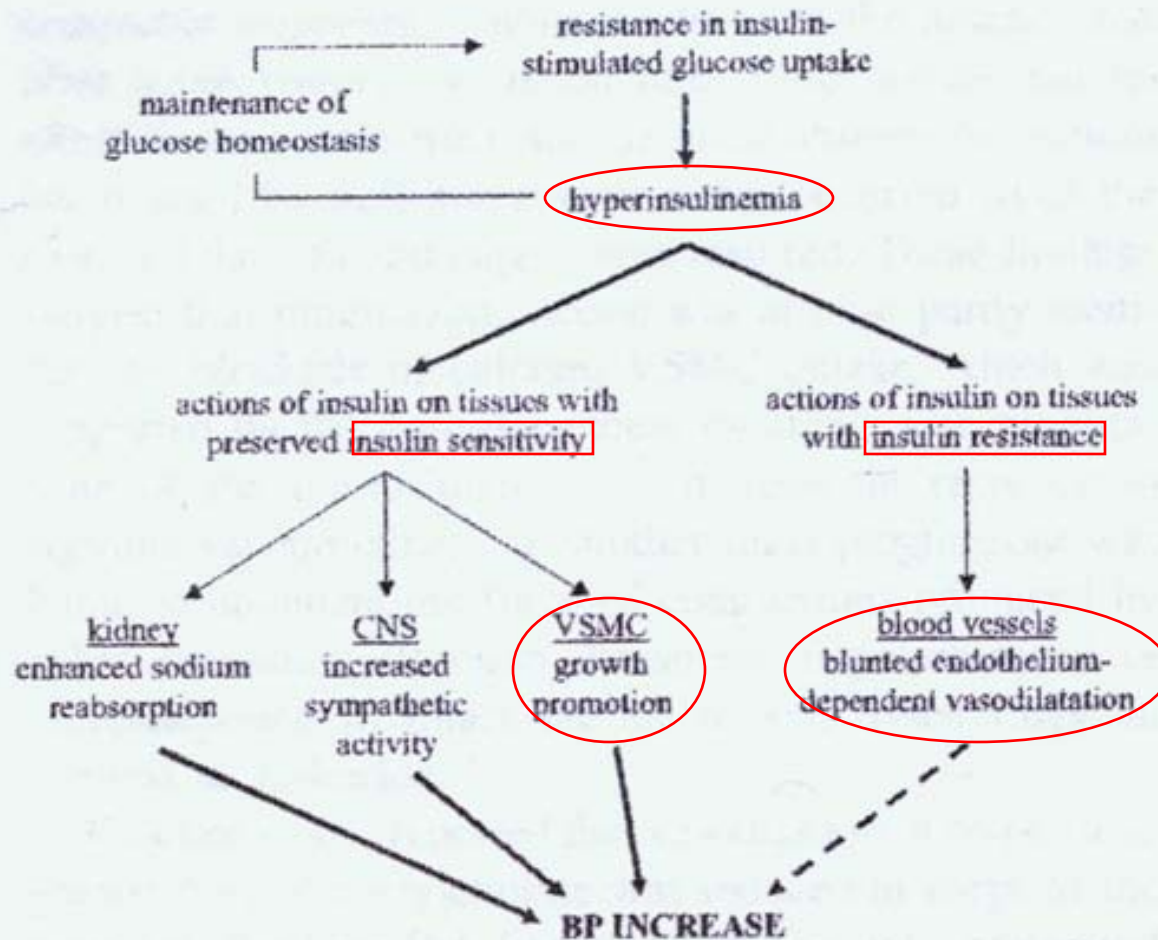


**FIG. 1.** Possible mechanisms connecting insulin resistance and compensatory hyperinsulinemia with increase in blood pressure (BP). CNS = central nervous system; VSMC = vascular smooth muscle cells.

## TGF $\beta$ AND DIABETIC NEPHROPATHY

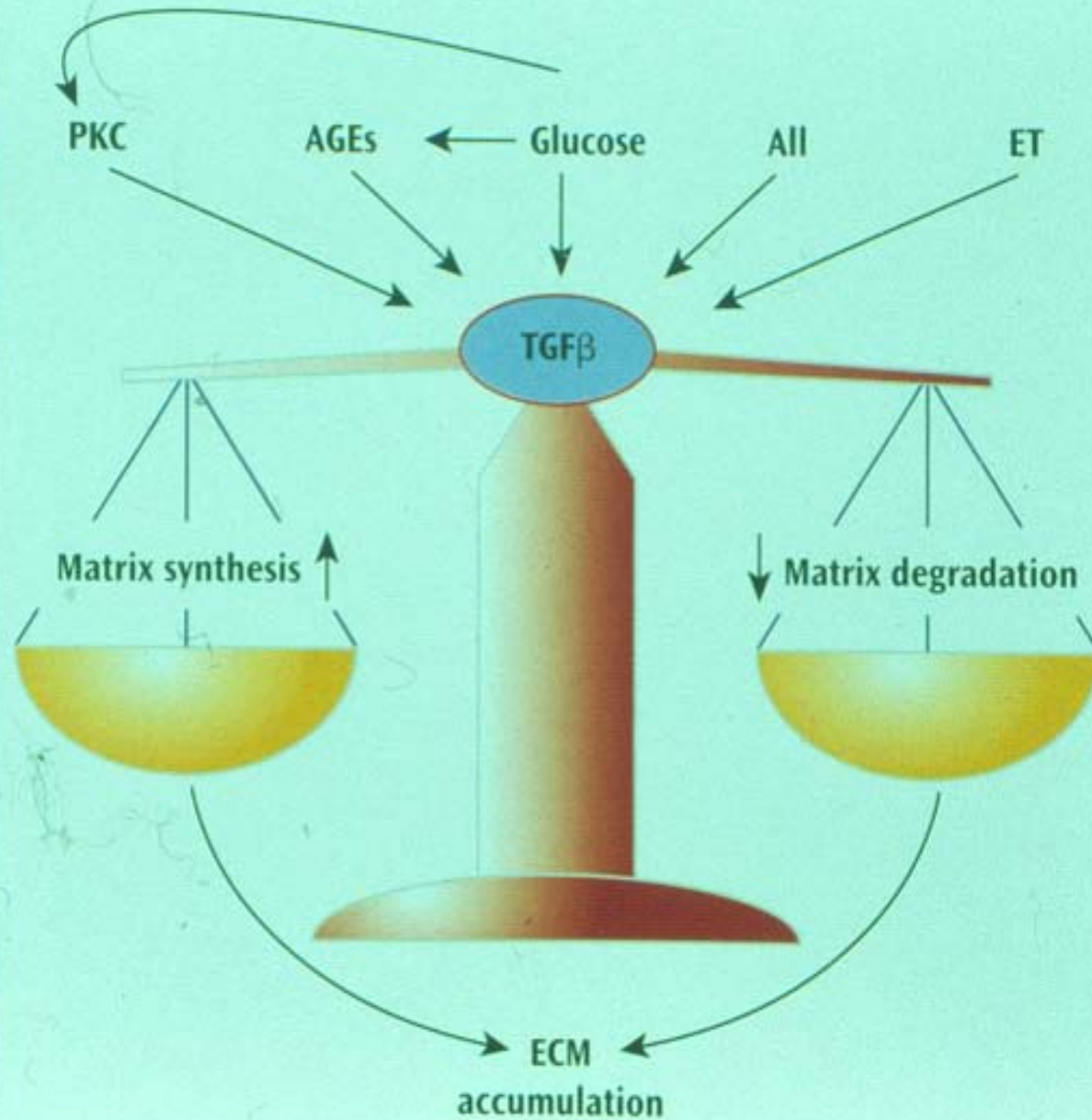
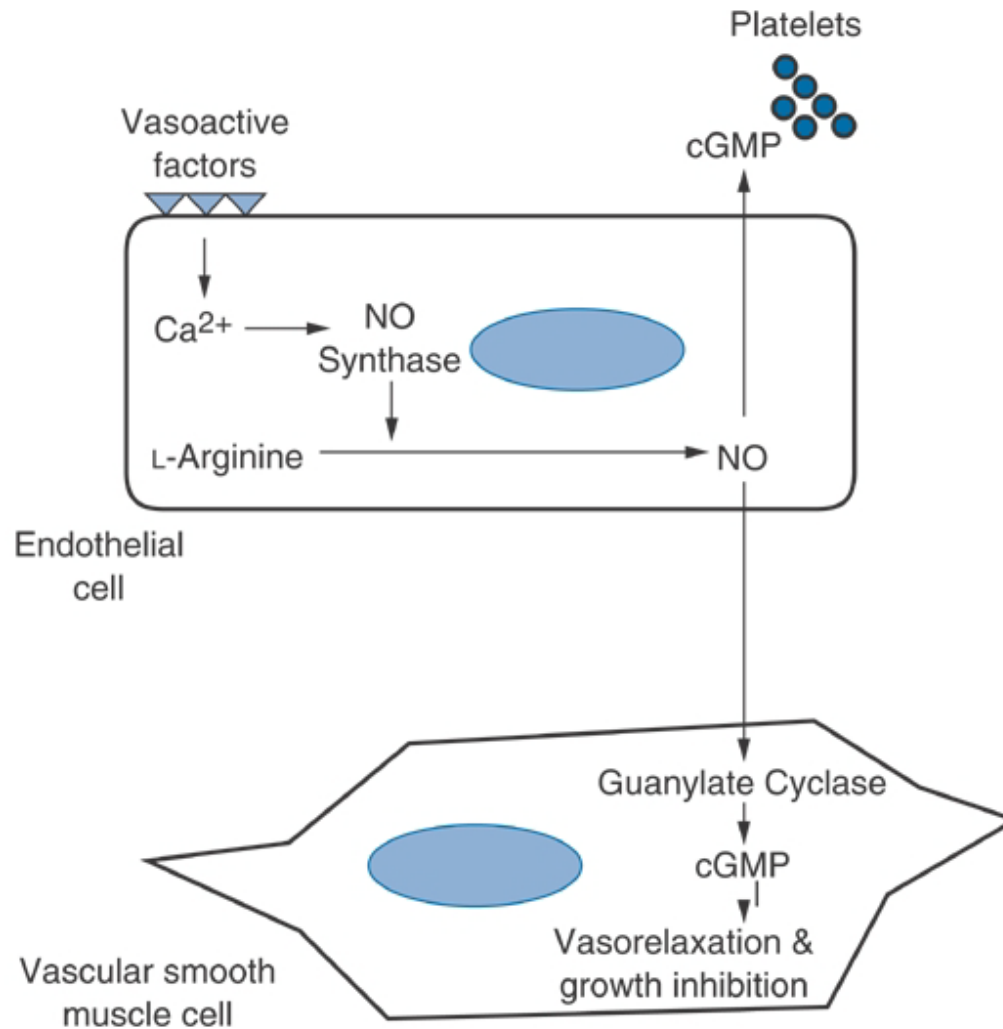
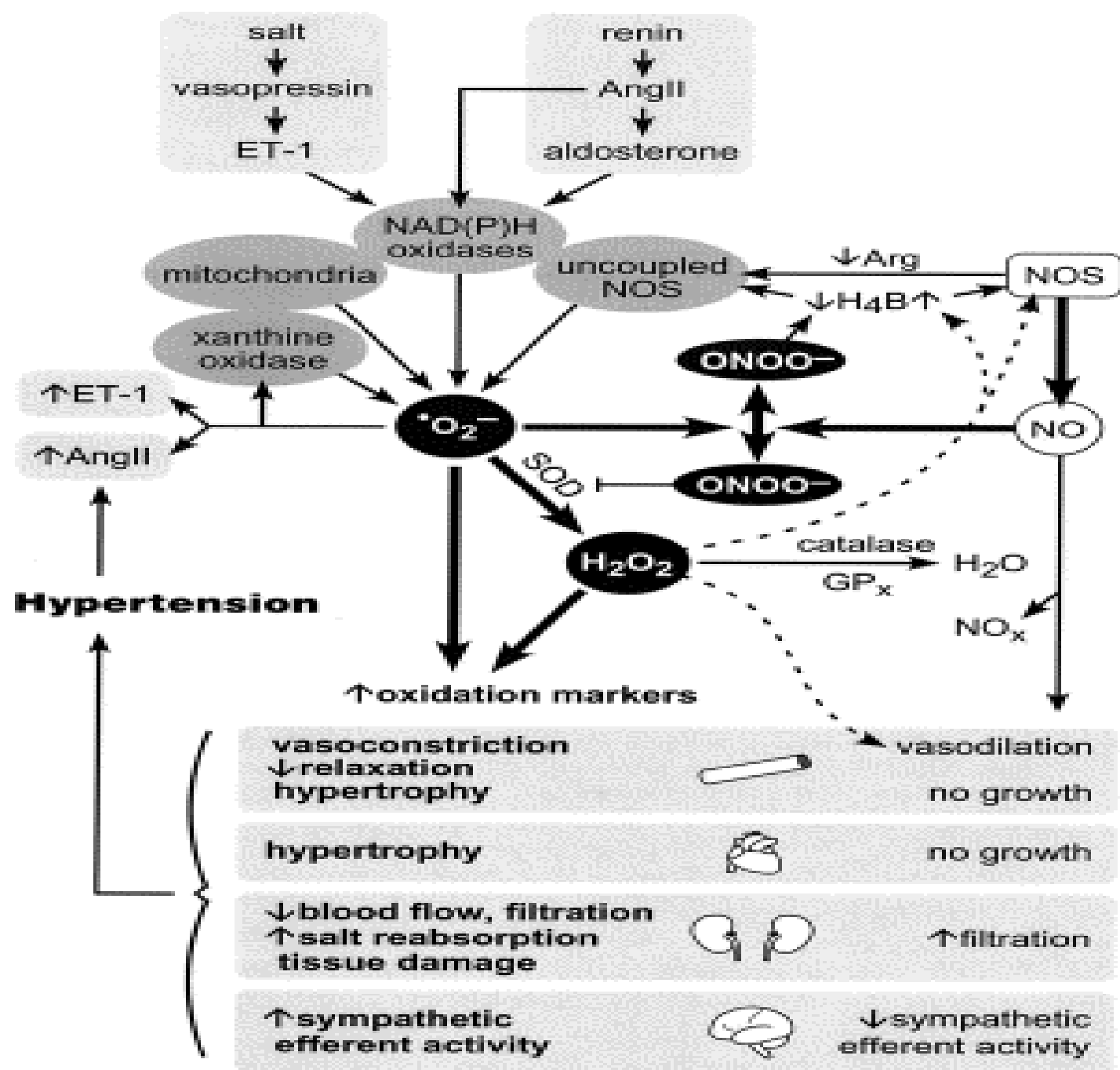


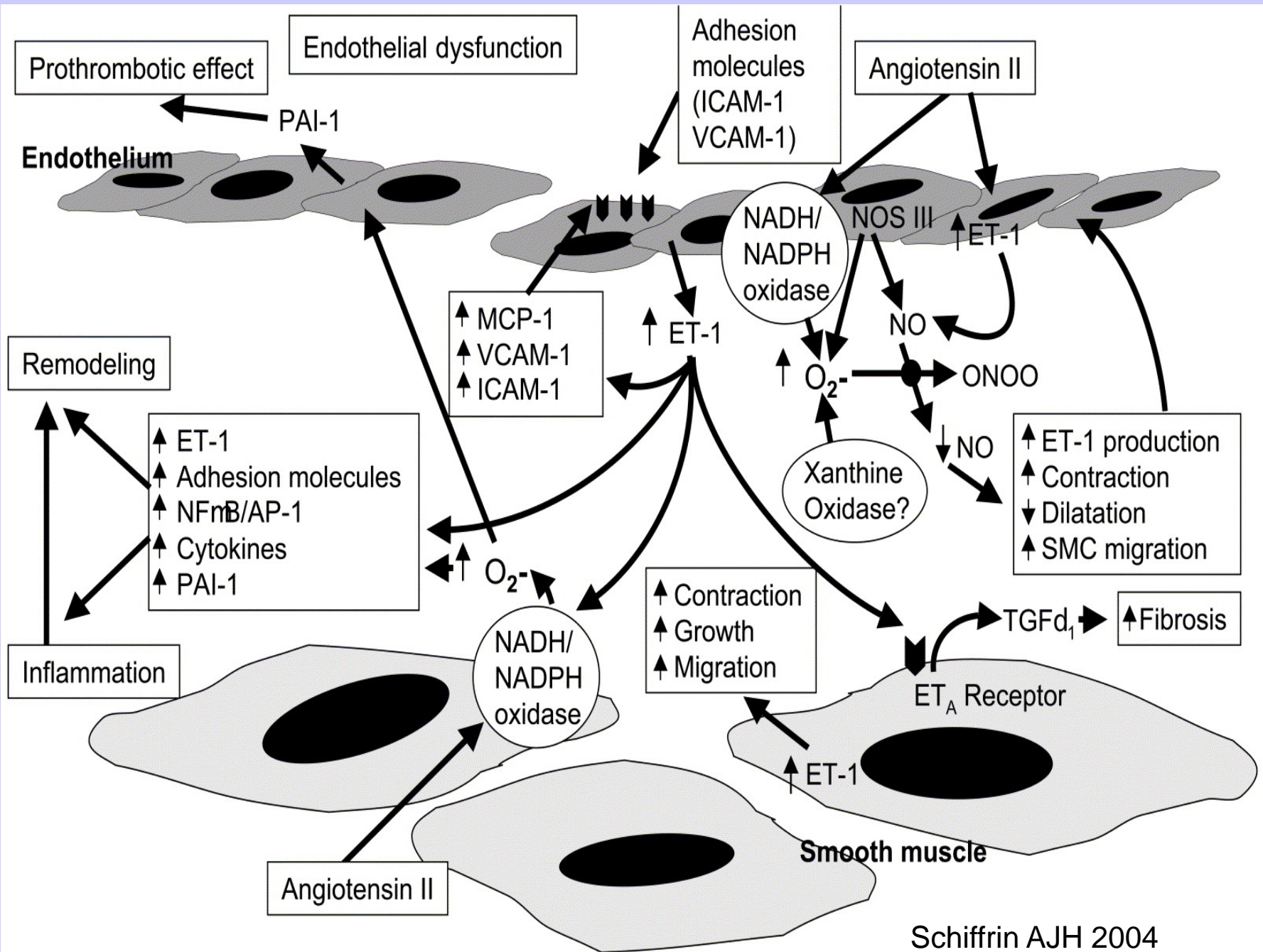
*Figure 7*  
Schema outlining multiple stimuli which may be activated in diabetes promotes extracellular matrix accumulation which promote expression of TGF $\beta$ , a growth factor which via increases in matrix synthesis and decreases in matrix degradation.

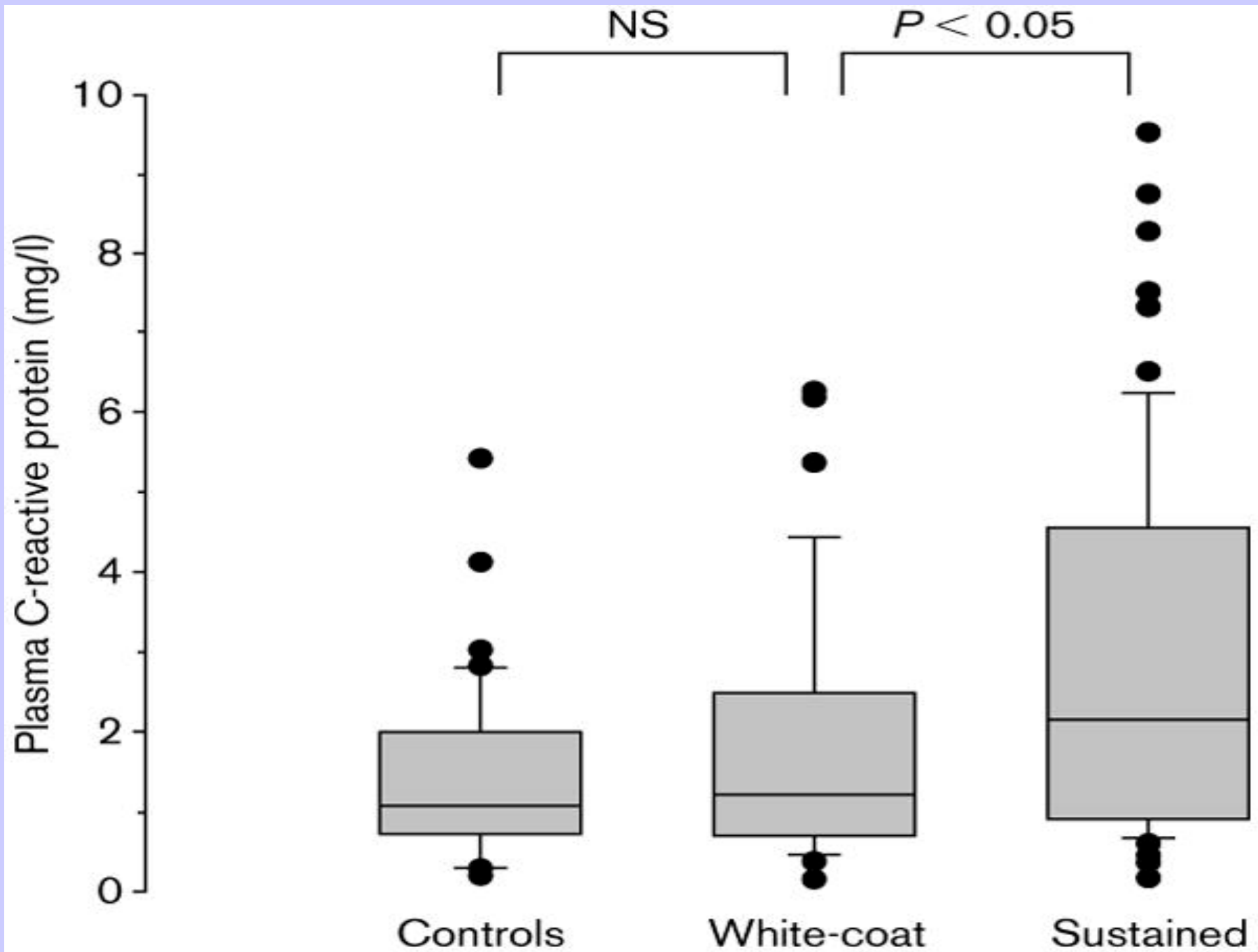


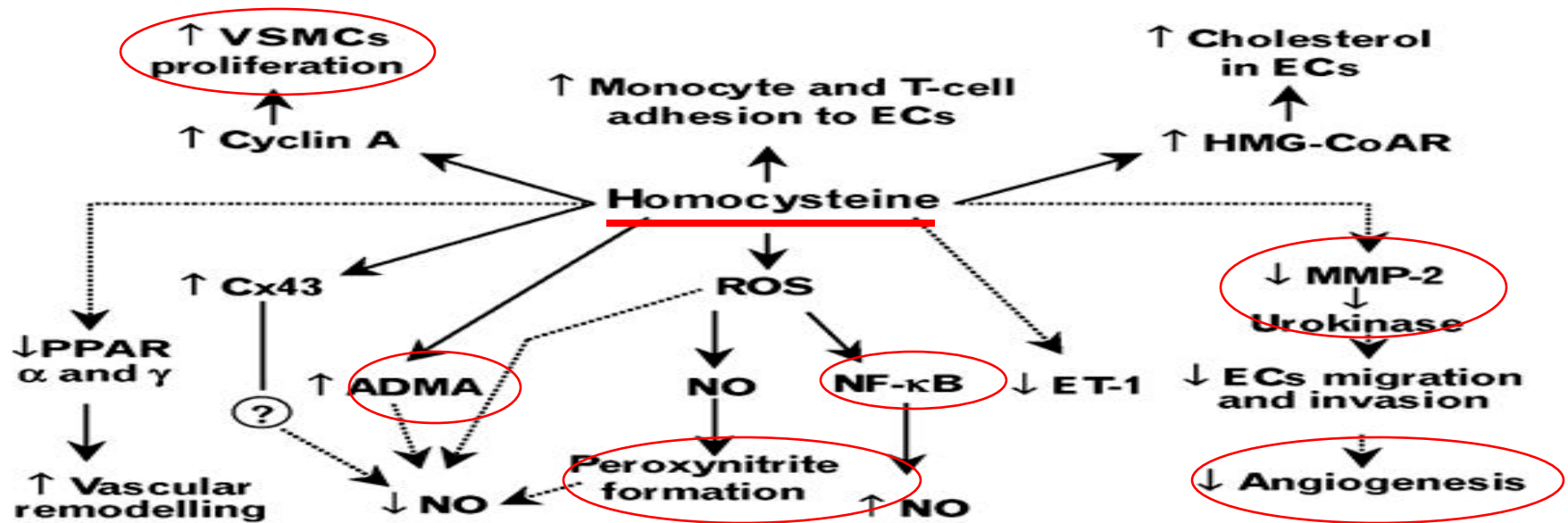
Nitric oxide (NO) is an important regulator of vessel wall function. In response to a variety of vasoactive factors, including increased fluid shear stress, endothelial cells activate NO synthase, which generates NO from L-arginine. NO diffuses rapidly from the cell and activates guanylate cyclase in target cells. In platelets, this inhibits aggregation; in smooth muscle, it causes vasorelaxation and growth inhibition. cGMP, cyclic guanosine monophosphate.





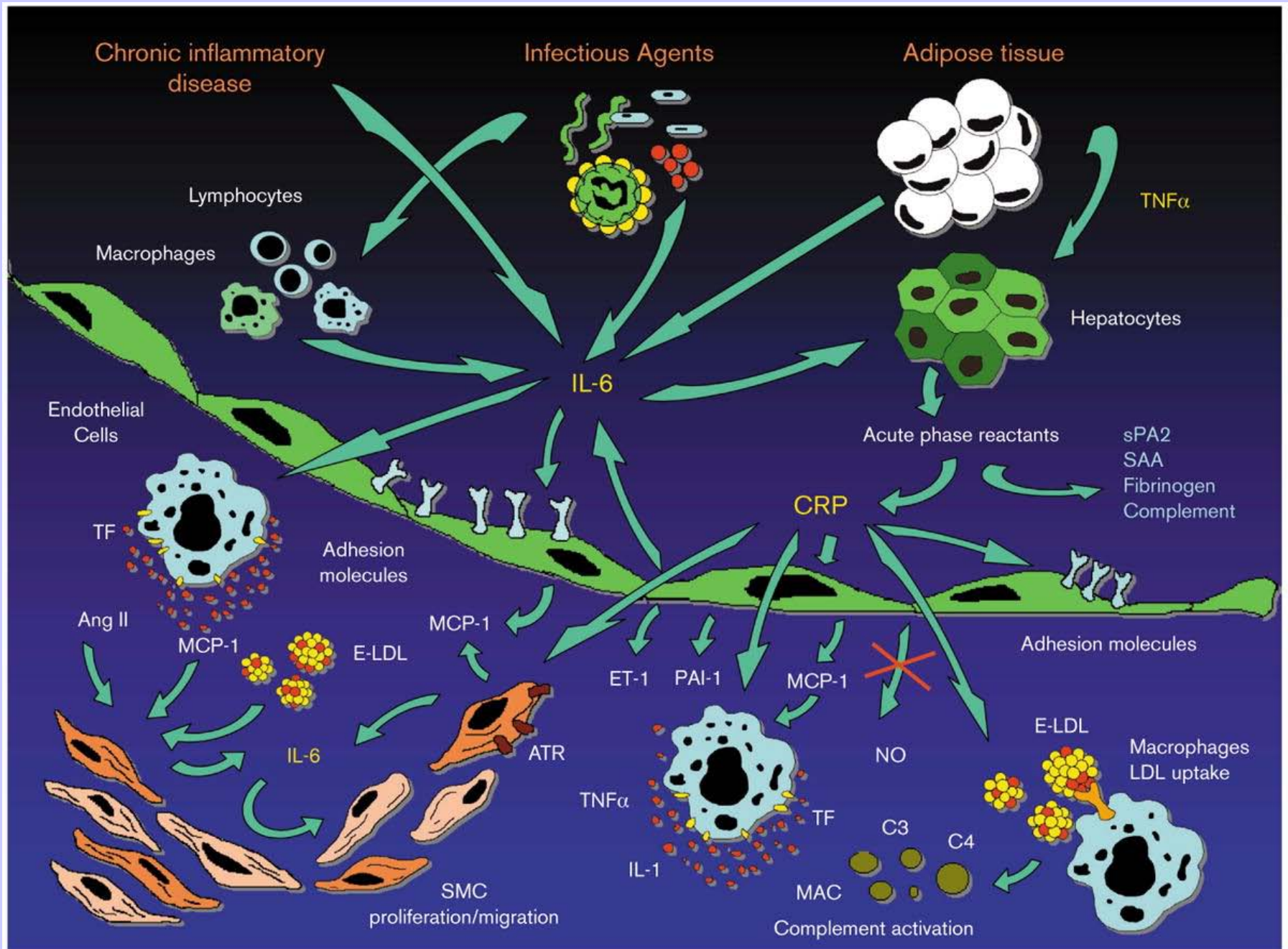


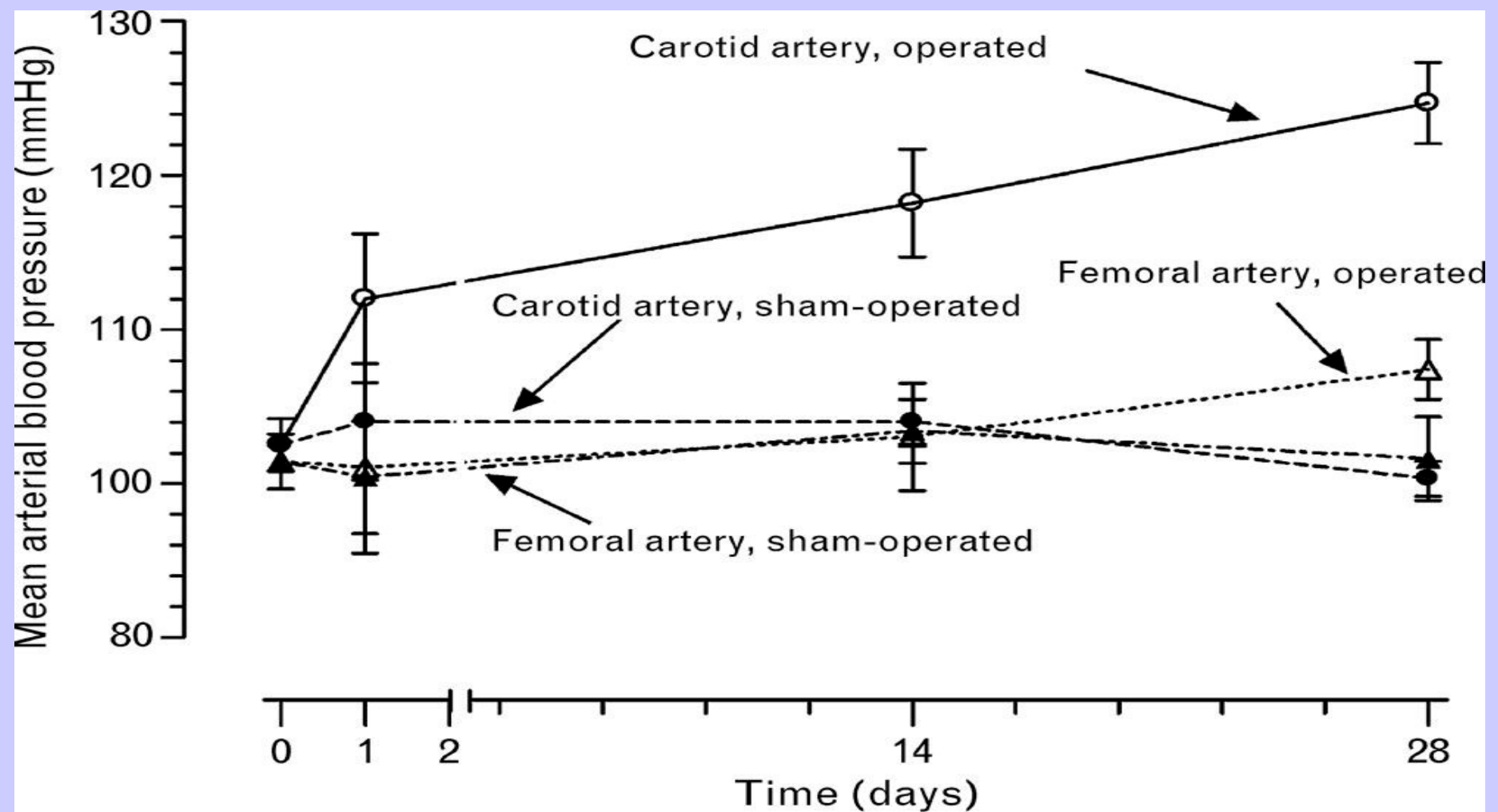




Schematic representation of the mechanisms by which hyperhomocysteinaemia can adversely affect endothelial function (continuous and dotted lines indicate stimulation and inhibition, respectively). Homocysteine, a sulphur-containing amino acid, can undergo auto-oxidation, thus generating the potent ROS superoxide anion, which reacts with nitric oxide (NO) to generate peroxynitrite. Homocysteine was shown to increase the endogenous endothelial nitric oxide synthase inhibitor, asymmetric dimethylarginine (ADMA), that contributes to decreasing the availability of nitric oxide. Hyperhomocysteinaemia was also shown to increase cholesterol in human umbilical vein endothelial cells (ECs) by enhancing the expression of 3-hydroxy-3-methylglutaryl coenzyme A reductase (HMG-CoAR). Thus increased local generation of cholesterol in endothelial cells, as a result of oxidative stress, may be an additional mechanism contributing to endothelial dysfunction. Additional mechanisms of vascular damage entail blunting of peroxisome proliferator-activated receptors (PPAR),  $\alpha$  and  $\gamma$ , stimulation of cyclin A and paradoxical overexpression and translocation of connexin 43 (Cx43). Homocysteine was also shown to increase the adhesion of monocytes and T cells to human aortic endothelial cells and to enhance the expression of adhesins on the endothelial surface and their mRNA levels. VSMCs, vascular smooth muscle cells; MMP, matrix metalloproteinase; NF- $\kappa$ B, nuclear factor- $\kappa$ B; ET-1, endothelin-1.

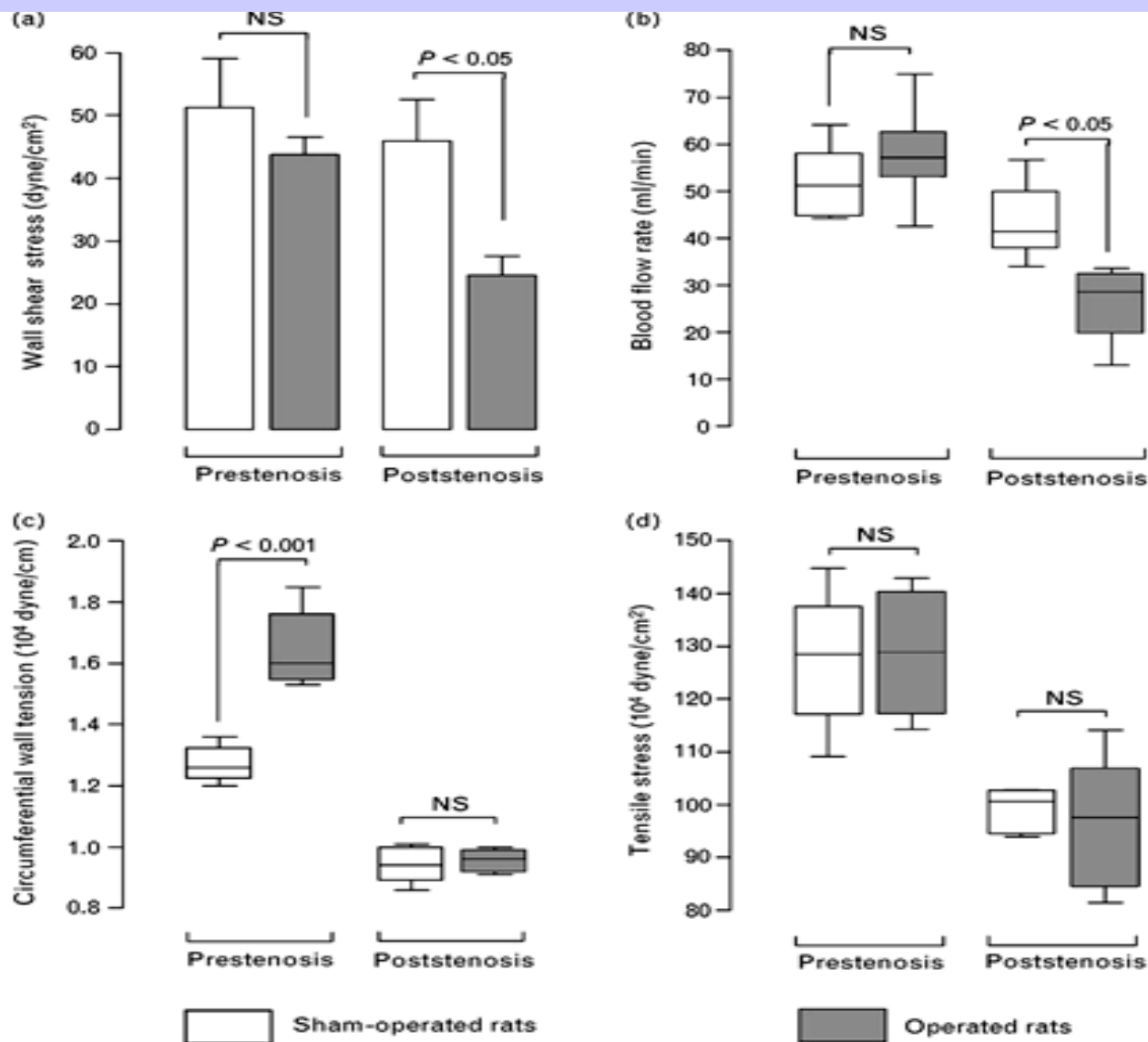




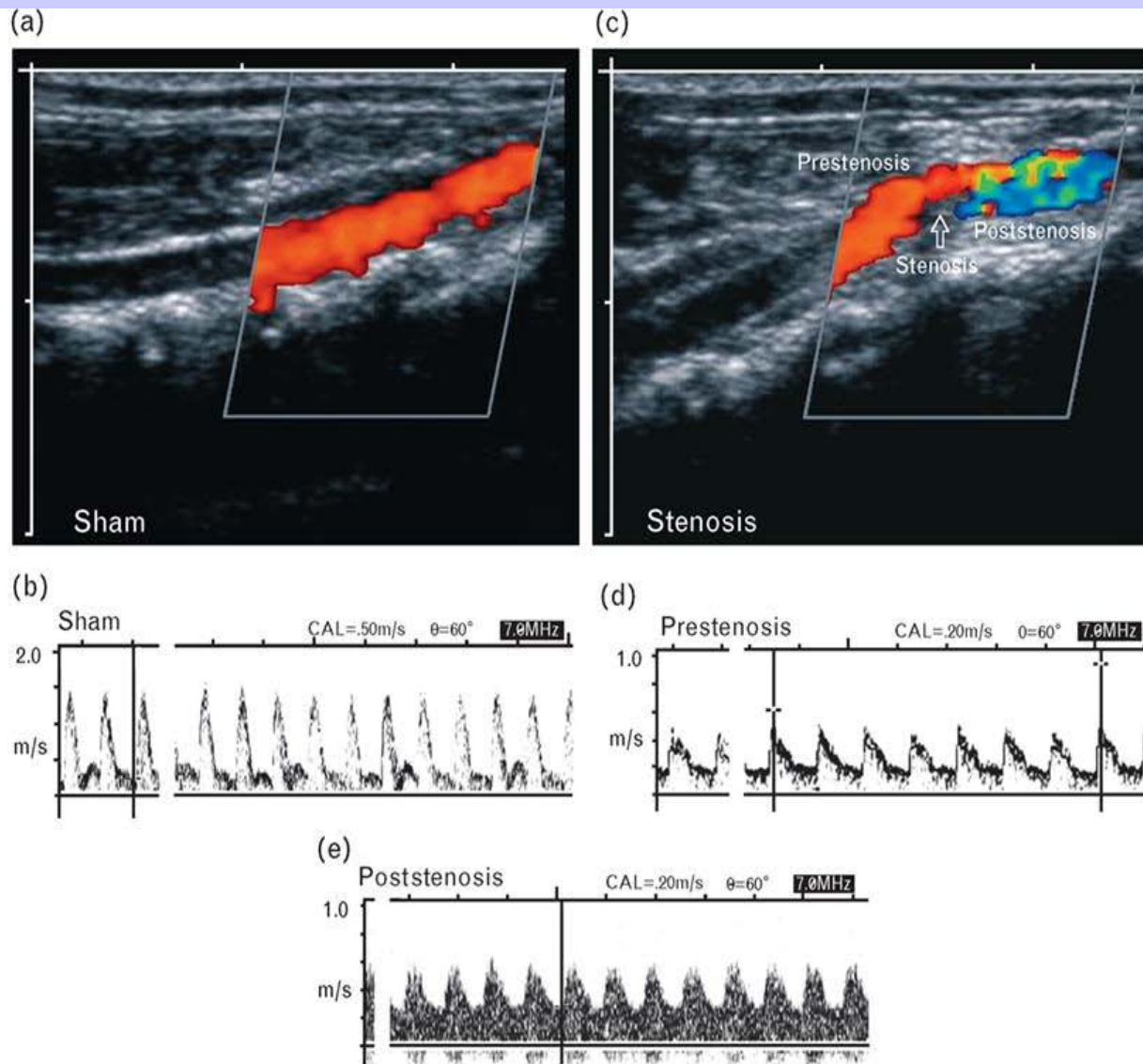


Mean carotid and femoral blood pressures in operated and sham-operated rats during the 28-day period of study. The mean carotid blood pressure of constricted rats reached a maximum at the 4th week. The mean femoral blood pressure in operated animals was comparable to the mean carotid and femoral blood pressures in sham-operated controls.



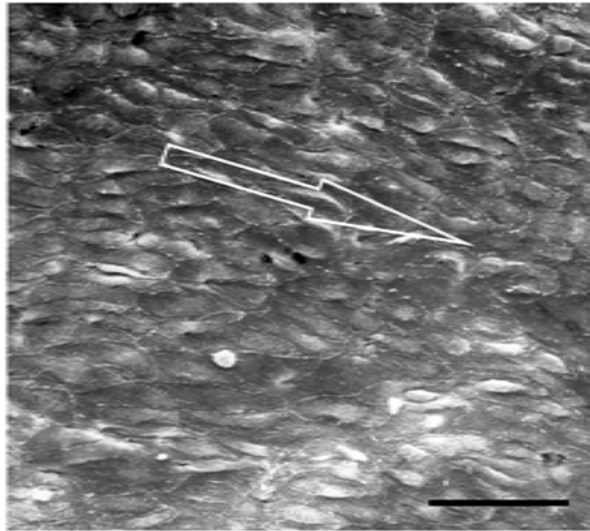


(a) Wall shear stress mean values (dyne/cm<sup>2</sup>) in sham-operated and prestenotic and poststenotic aortas at day 28 of the experiment. (b) Blood flow rate (ml/min). Box and whisker graph shows the batches of data in sham-operated and prestenotic and poststenotic aortas at day 28 of the experiment. (c) Circumferential wall tension (10<sup>4</sup> dyne/cm). Box and whisker graph show the batches of data in sham-operated and prestenotic and poststenotic aortas at day 28 of the experiment. The mean circumferential wall tension (CWT) level in the prestenotic segments increased in comparison to that of corresponding segments from control aortas. The mean CWT value in the poststenotic segments were similar in both groups. (d) Tensile stress (10<sup>4</sup> dyne/cm<sup>2</sup>). Box and whisker graph show the batches of data in sham-operated and prestenotic and poststenotic aortas at day 28 of the experiment. The means tensile stresses (TS) in both prestenotic and poststenotic segments were similar to those in the corresponding segments from control aortas.

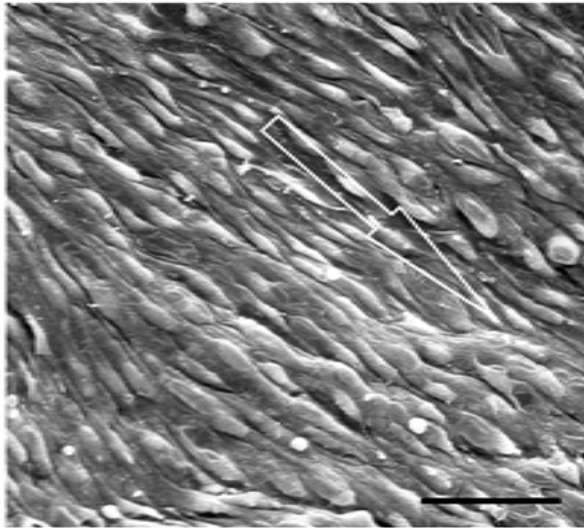


Color Doppler shows a laminar flow in the control aorta (a), whereas the spectrum of this laminar flow is characterized by a clear systolic window (b). Color Doppler in operated rats demonstrates a preserved laminar flow in the prestenotic segment and a mixed red and blue poststenotic segment characterizing turbulent flow (c). In the prestenotic segment the Doppler spectrum showed a laminar flow with relative lower resistance (d), whereas a spectral broadening Doppler, the hallmark of turbulent flow, could be demonstrated in the poststenotic segment (e).

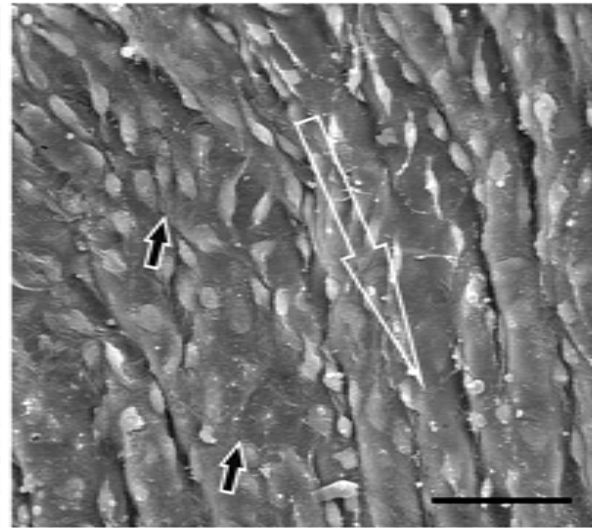
Sham



Prestenosis

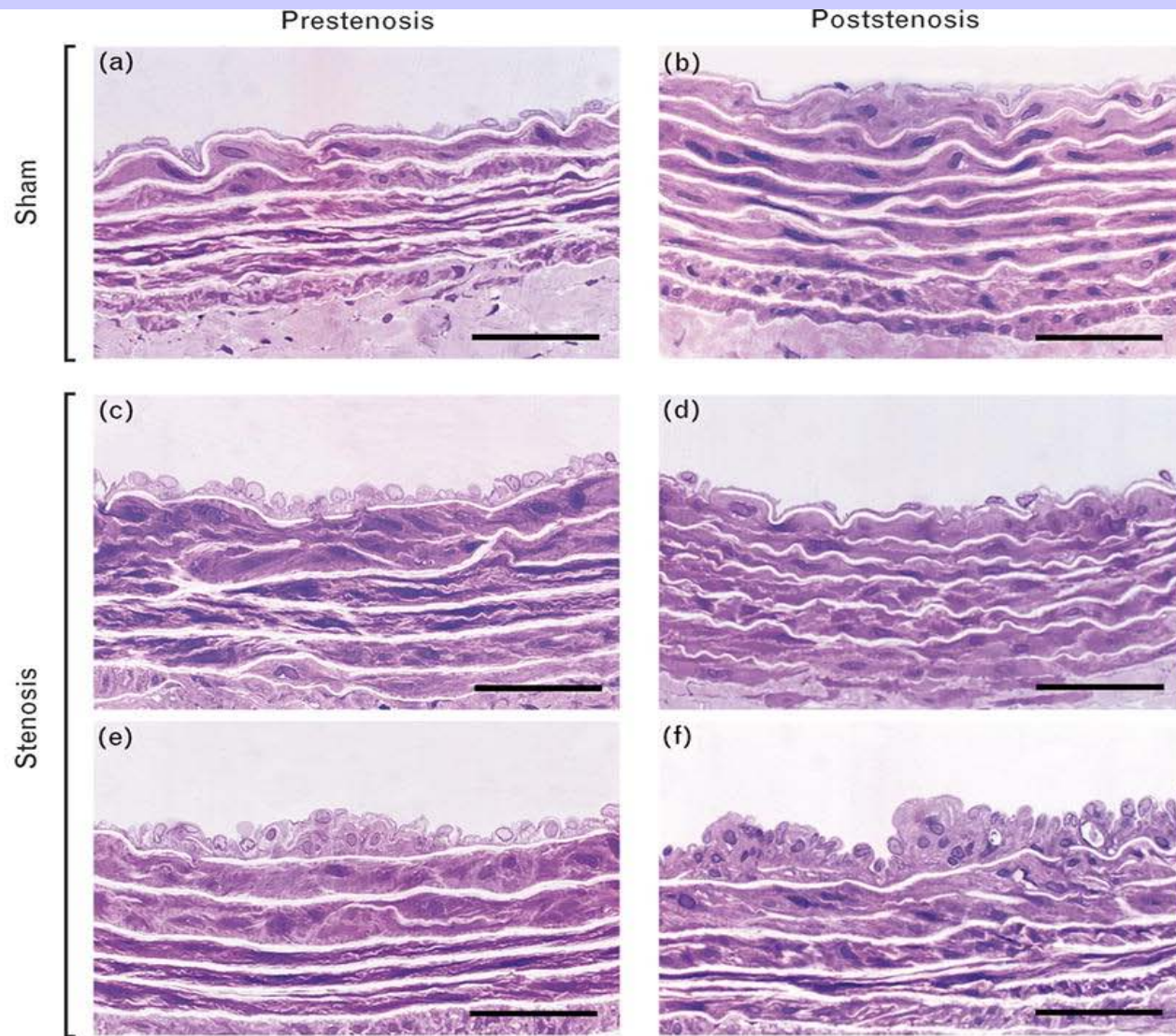


Poststenosis

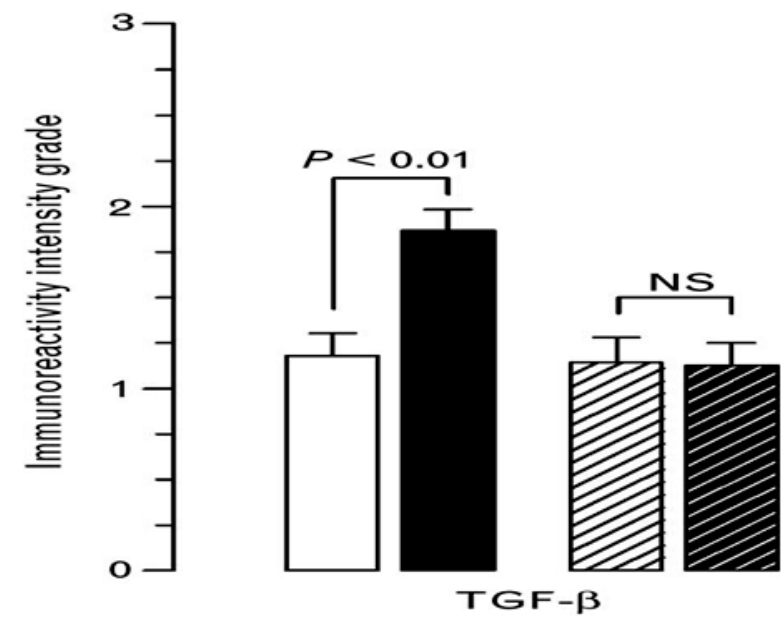
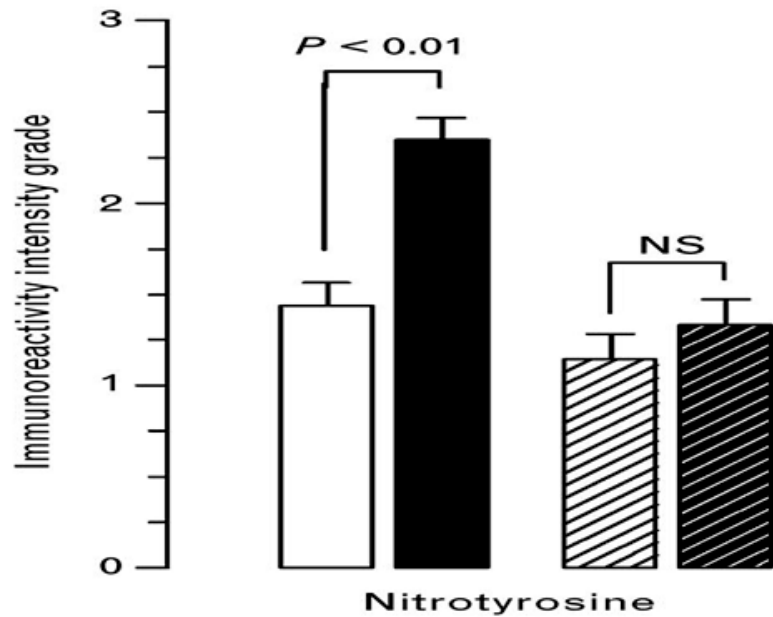
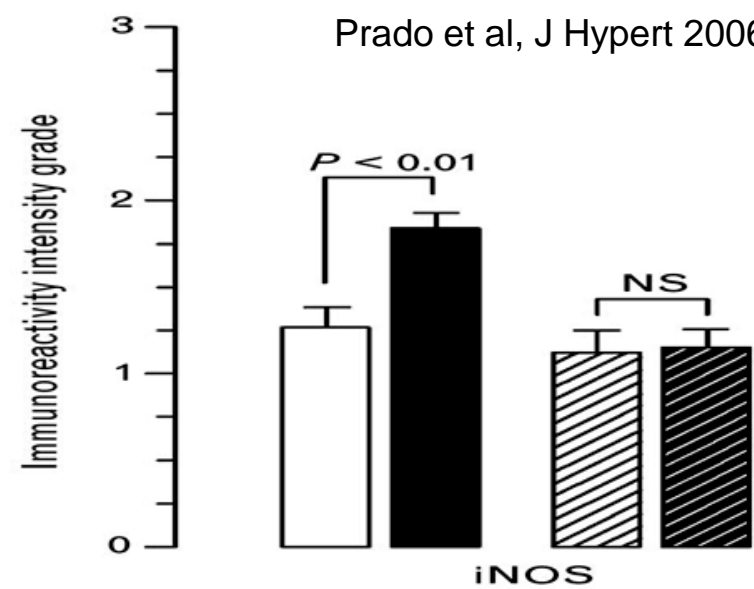
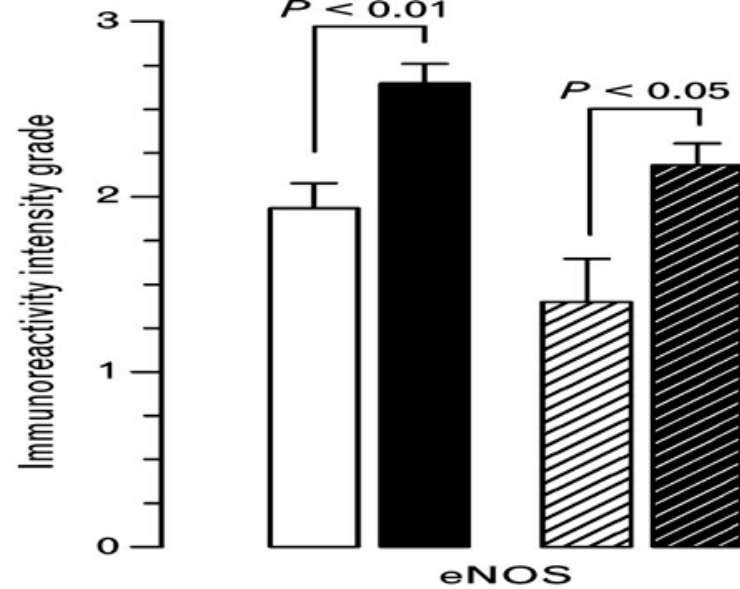


Scanning electron microscopy. Representative views of the endothelial surface in sham-operated animals showing typical cobblestone morphology with major axis parallel to the direction of the blood flow (large open arrow). The prestenotic segment shows more voluminous and elongated endothelial cells with the major axis in the direction of the blood flow (large open arrow). The endothelial cells in the poststenotic segment are non-directional in relation to the direction of the blood flow (large open arrow) with many polygonal cells (closed small arrows). Scale bars, 40  $\mu\text{m}$ .



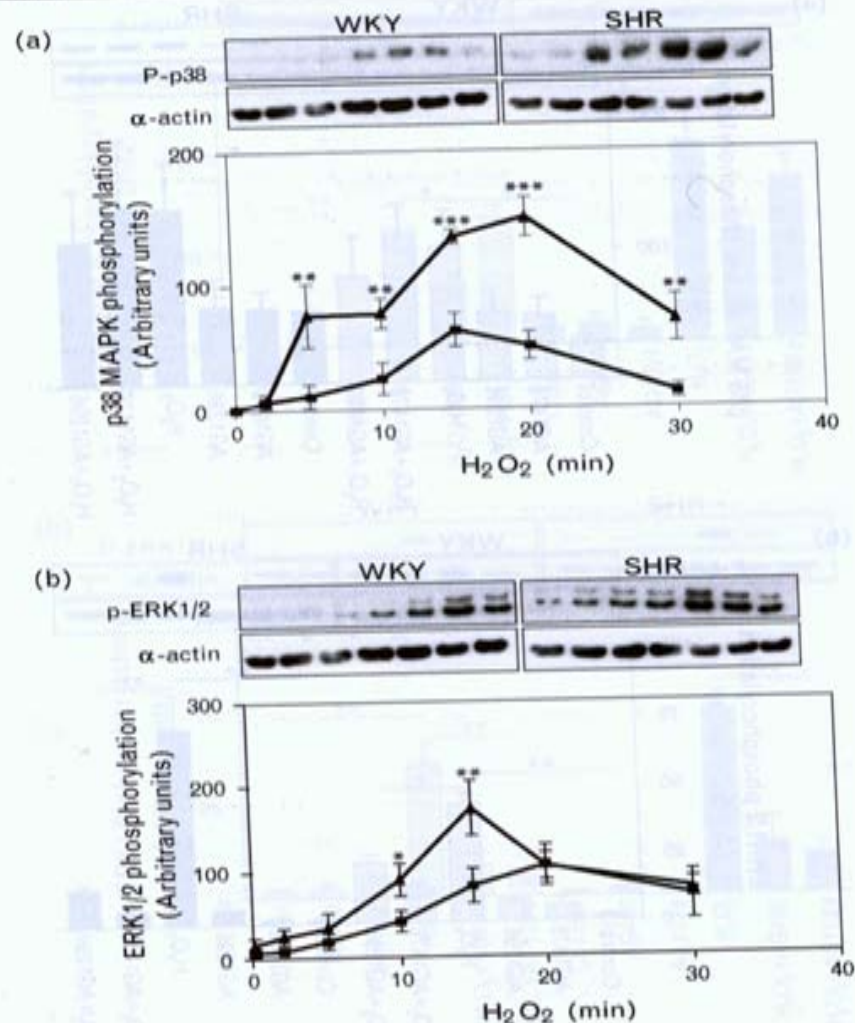


High resolution light microscopy. Representative views of the aortas from sham-operated rats (a and b) and prestenotic (c and e) and poststenotic (d and f) segments from operated rats. In the prestenotic segment there is diffuse intimal thickening with enlarged endothelial cells (c) and diffusely distributed minute foci of intimal thickening composed of smooth muscle cells and occasional mononuclear cells with collagen and elastic fibers surrounding them (e) and medial thickening (c and e), contrasting with the delicate structure of the intima in the control group (a). In the poststenotic segment the intima appears delicate (d), quite similar to the intima in the corresponding segment of the aorta in the control group (b), except for focally distributed areas of striking intimal thickening composed of smooth muscle cells and occasional mononuclear cells intermixed with basement membrane-like material, collagen and elastic fibres (f). Toluidine blue stain, transversal sections. Scale bars, 20  $\mu$ m (a–f).



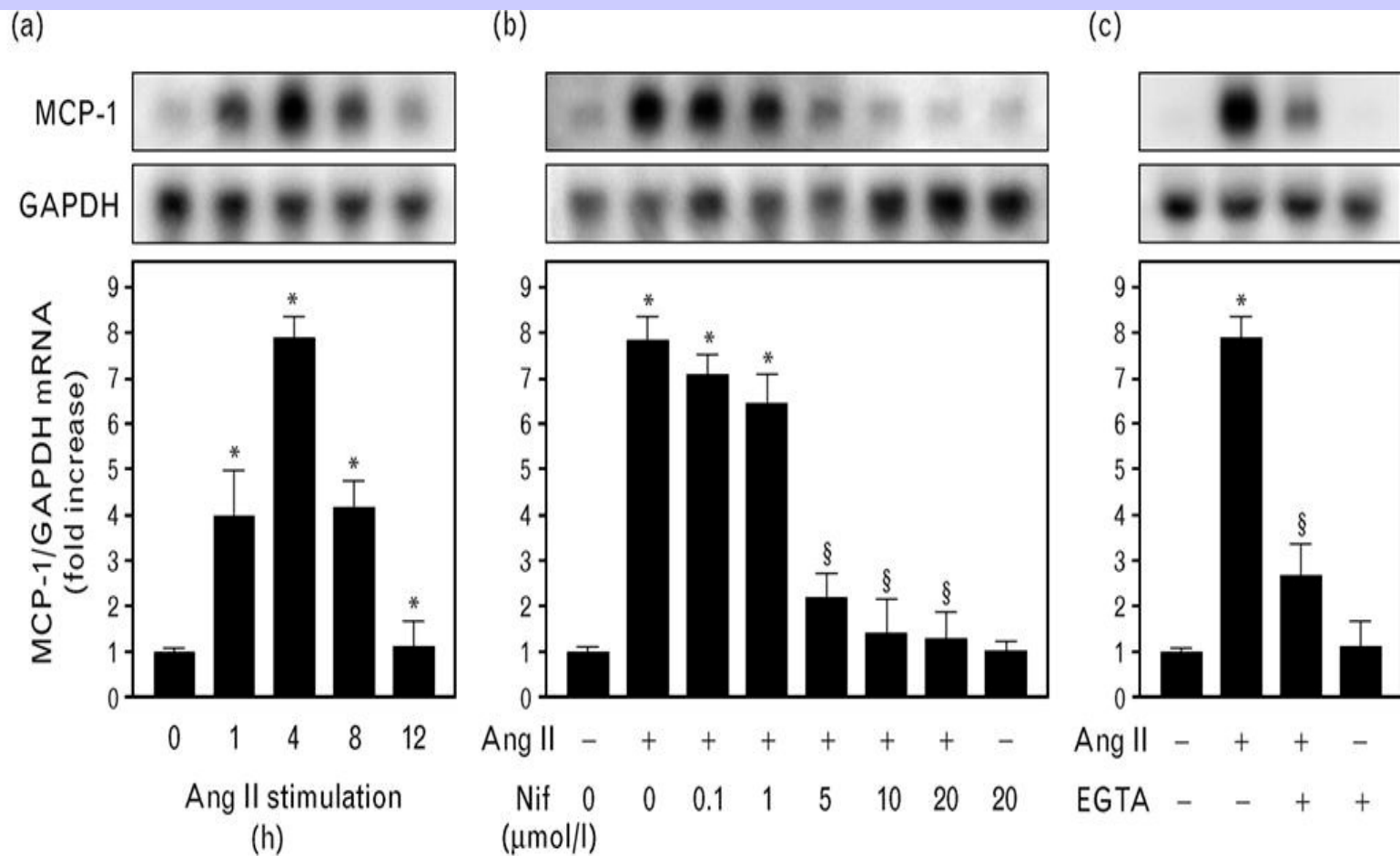
Quali-quantitative evaluation of the brown stained features [endothelial nitric oxide synthase (eNOS), inducible nitric oxide synthase (iNOS), nitrotyrosine, and transforming growth factor beta (TGF- $\beta$ )] in prestenotic and poststenotic segments of sham-operated and operated rats. □ Sham-prestenosis; ■ stenosis-prestenosis; ▨ sham-poststenosis; ▩ stenosis-poststenosis.



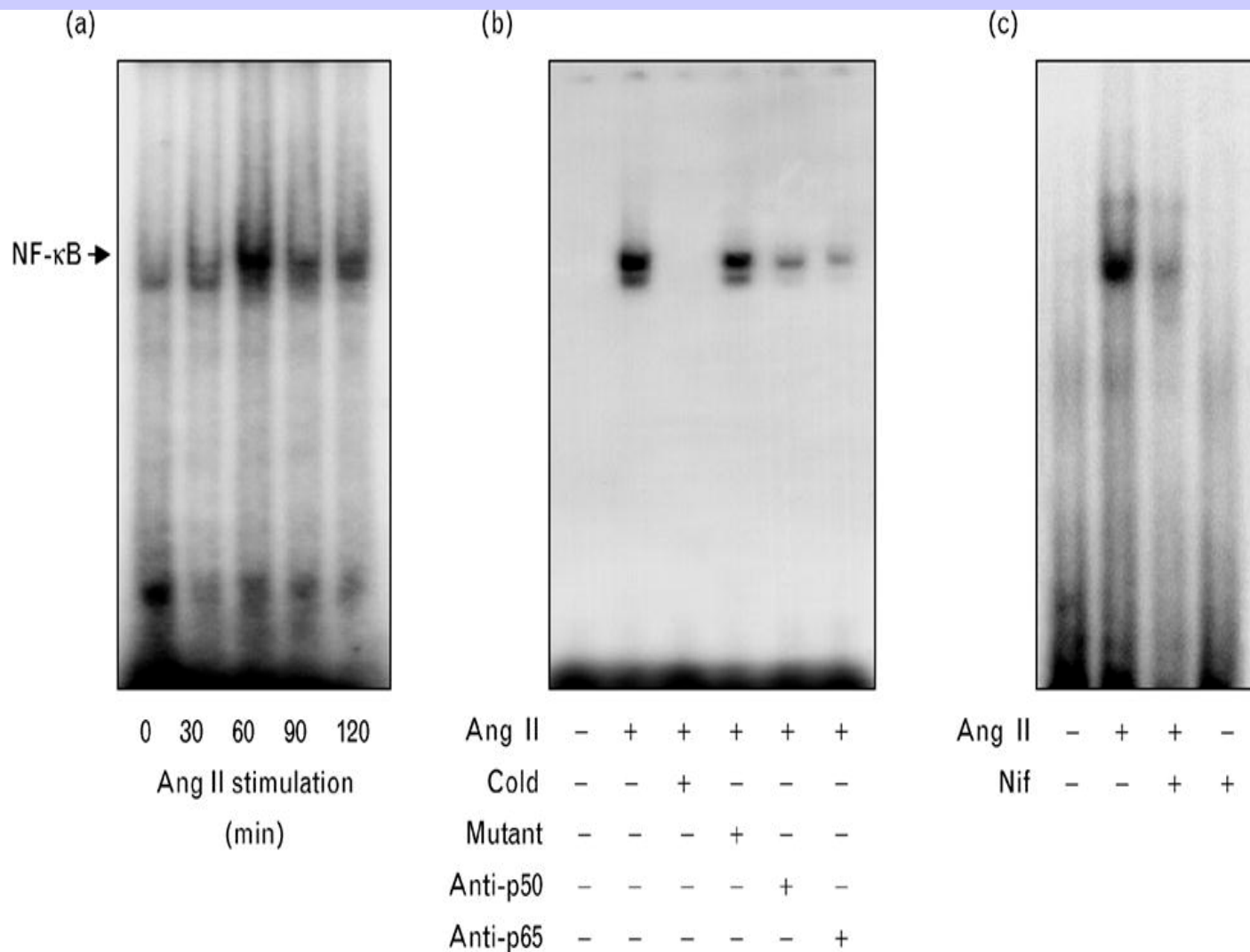
**Fig. 1**

Effect of hydrogen peroxide on extracellular signal-regulated kinases 1/2 and p38 mitogen-activated protein kinase phosphorylation in vascular smooth muscle cells from Wistar-Kyoto rats (WKY) and spontaneously hypertensive rats (SHR). Top panels are representative immunoblots of p38 mitogen-activated protein (MAP) kinase (a) and extracellular signal-regulated kinases (ERK) 1/2 (b) phosphorylation by hydrogen peroxide (H<sub>2</sub>O<sub>2</sub>) (10<sup>-4</sup> mol/l). Membranes were probed with phospho-specific antibodies and re-probed with anti- $\alpha$  actin antibody to assess protein loading. Line graph demonstrates time-dependent effect of H<sub>2</sub>O<sub>2</sub>. Each data point is the mean  $\pm$  SEM of five experiments. \* $P$  < 0.05, \*\* $P$  < 0.01, \*\*\* $P$  < 0.001 versus WKY counterpart. —■— WKY; —▲— SHR.



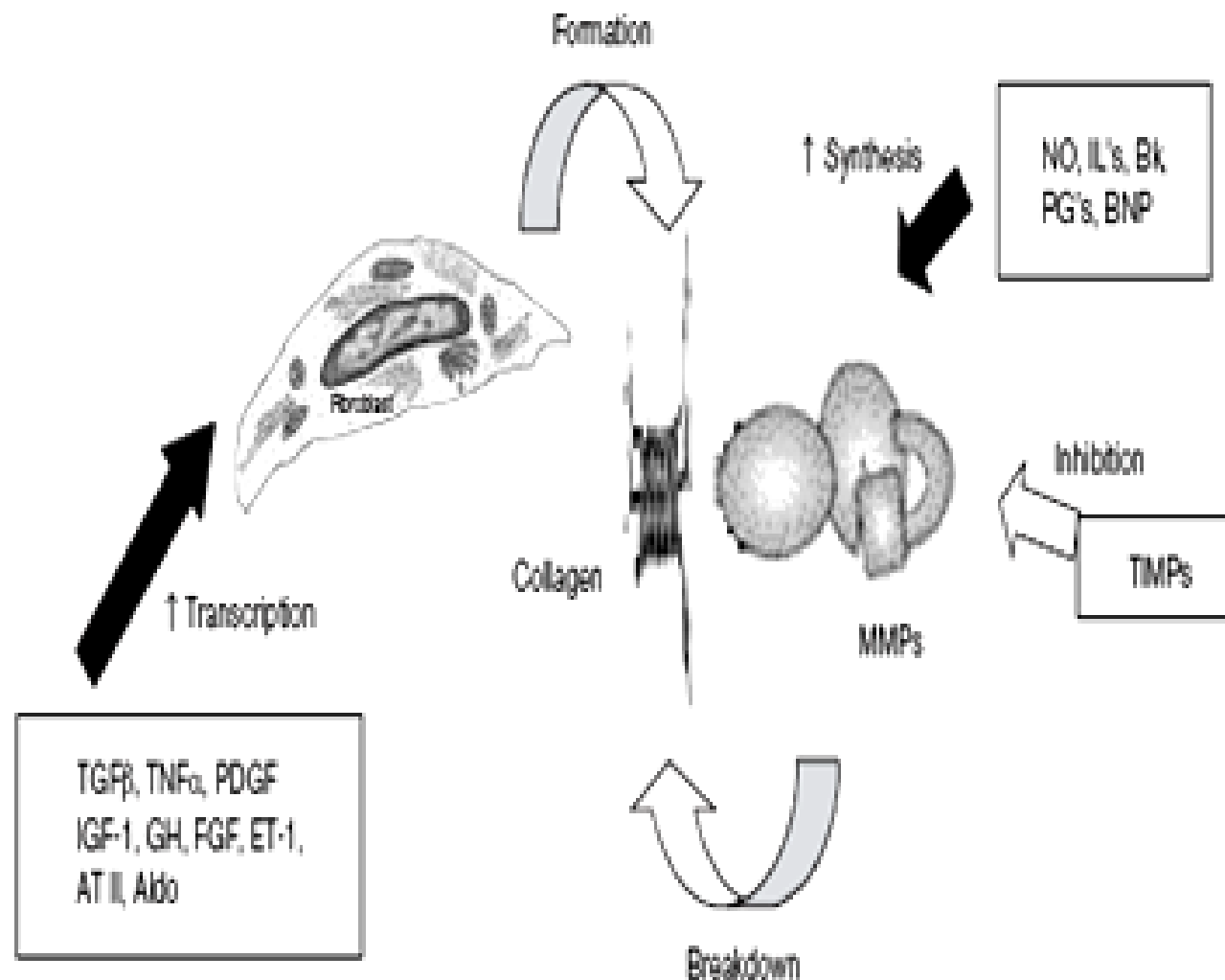


Effect of nifedipine on monocyte chemoattractant protein 1 (MCP-1) mRNA expression induced by angiotensin II in rat vascular smooth muscle cells (VSMC). Rat VSMC were cultured as described in the Methods section. Subconfluent cells were incubated in serum-free Dulbecco's modified Eagle's medium (DMEM) for 24 h before the experiment. MCP-1 mRNA was determined by Northern blot. RNA (25  $\mu\text{g/lane}$ ) was separated by electrophoresis, and hybridized with a probe for MCP-1. Glyceraldehyde-3-phosphate dehydrogenase (GAPDH) mRNA was used as an internal control. (a) Time course of MCP-1 mRNA expression in response to angiotensin II (Ang II) stimulation. (b) Effect of nifedipine on MCP-1 mRNA expression. Total RNA was prepared after 4 h of treatment with Ang II, with or without nifedipine. (c) Effect of EGTA on MCP-1 mRNA expression. Total RNA was prepared after 4 h of treatment with Ang II, with or without EGTA. Values are mean  $\pm$  SE of densitometric measurements ( $n = 4$ ). Similar results were obtained in eight different culture lines. Ang II,  $10^{-7}$  mol/l angiotensin II; Nif, nifedipine; EGTA, 0.5 mmol/l EGTA. \* $P < 0.05$  versus control;  $\S P < 0.05$  versus Ang II alone.

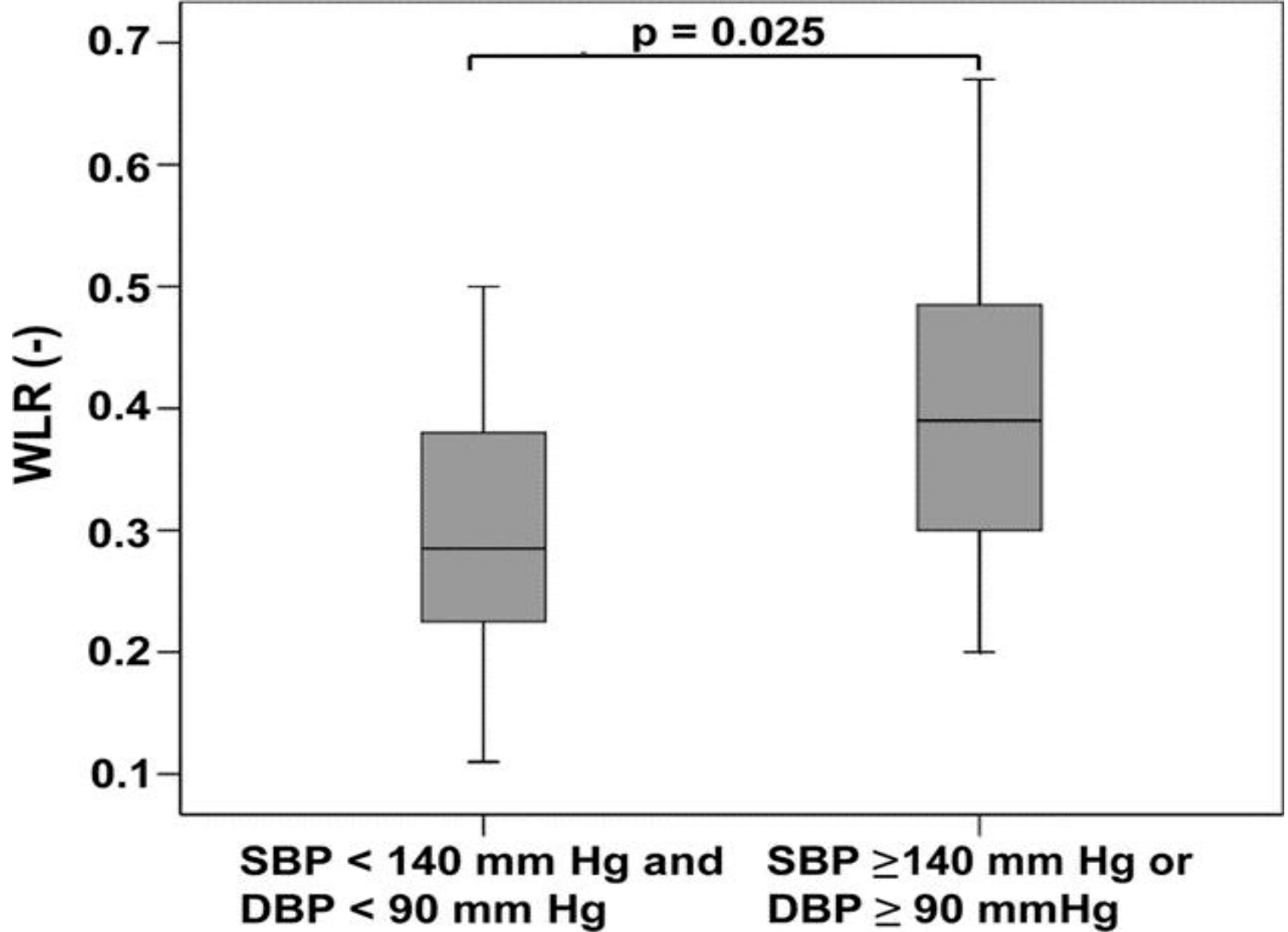


Effect of nifedipine on DNA binding activity of nuclear factor kappa B (NF-κB) induced by angiotensin II (Ang II). DNA binding activity of NF-κB was assayed by electrophoretic mobility shift assay with <sup>32</sup>P-labeled NF-κB binding oligonucleotide with nuclear extracts (10 μg) prepared from rat vascular smooth muscle cells (VSMC) as described in the Methods section. (a) Time course of DNA binding activity of NF-κB induced by Ang II. (b) DNA binding activity of NF-κB induced after 60-min stimulation by Ang II with unlabeled NF-κB, mutant NF-κB or anti-p65 or anti-p50 antibodies. (c) Effect of nifedipine on DNA binding activation of NF-κB induced by Ang II. Ang II, 10<sup>-7</sup> mol/l angiotensin II; Nif, 5 μmol/l nifedipine; similar results were obtained in five different culture lines.

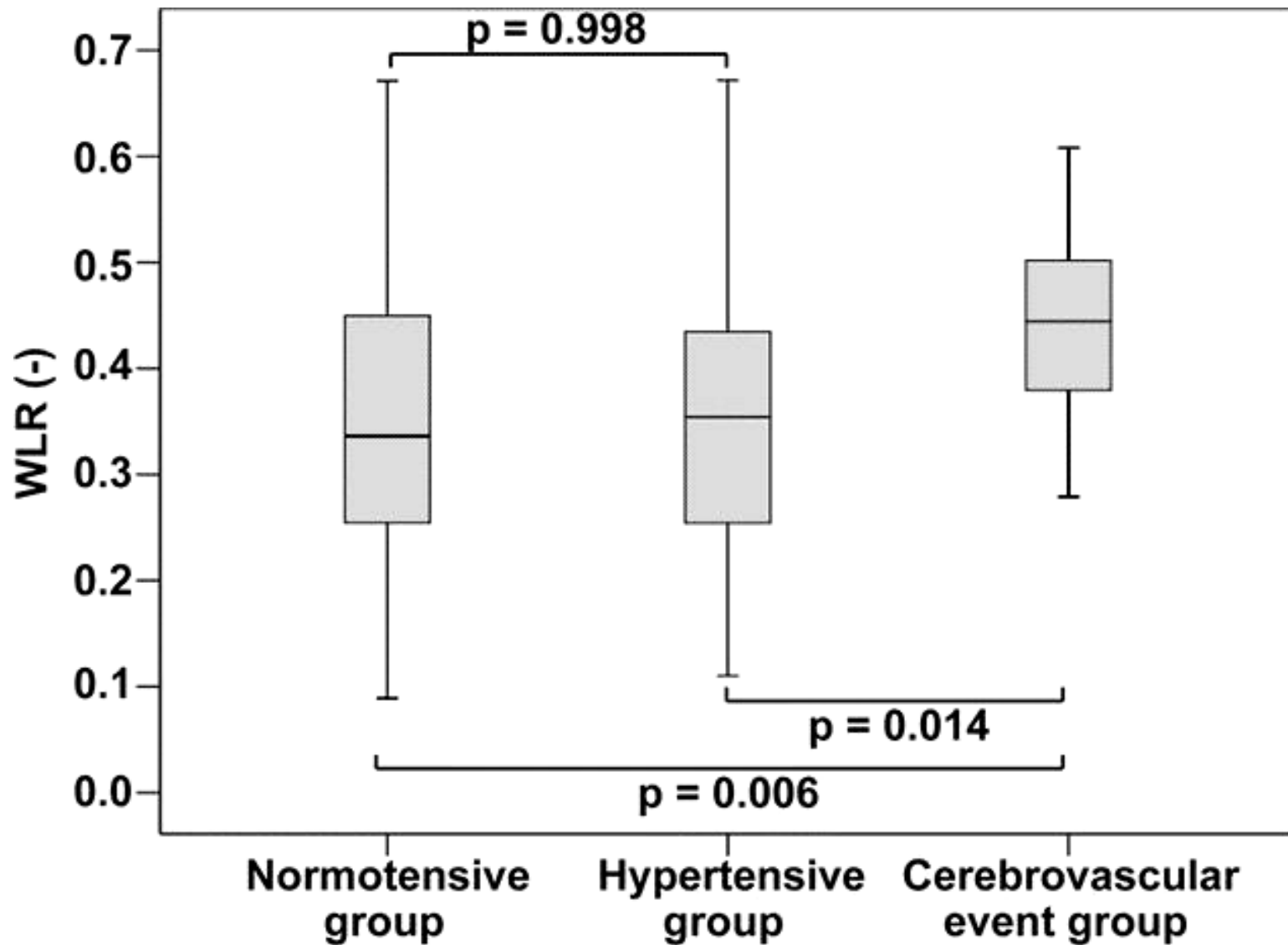




Mechanisms behind the synthesis and breakdown of collagen. NO, nitric oxide; IL, interleukin; Bk, bradykinin; PG, prostaglandin; BNP, brain natriuretic peptide; TIMP, tissue inhibitor of metalloproteinase; MMP, matrix metalloproteinase; TGF, transforming growth factor; TNF, tumour necrosis factor; PDGF, platelet-derived growth factor; IGF, insulin-like growth factor; GH, growth hormone; FGF, fibroblast growth factor; ET, endothelin; AT, angiotensin; Aldo, aldosterone.



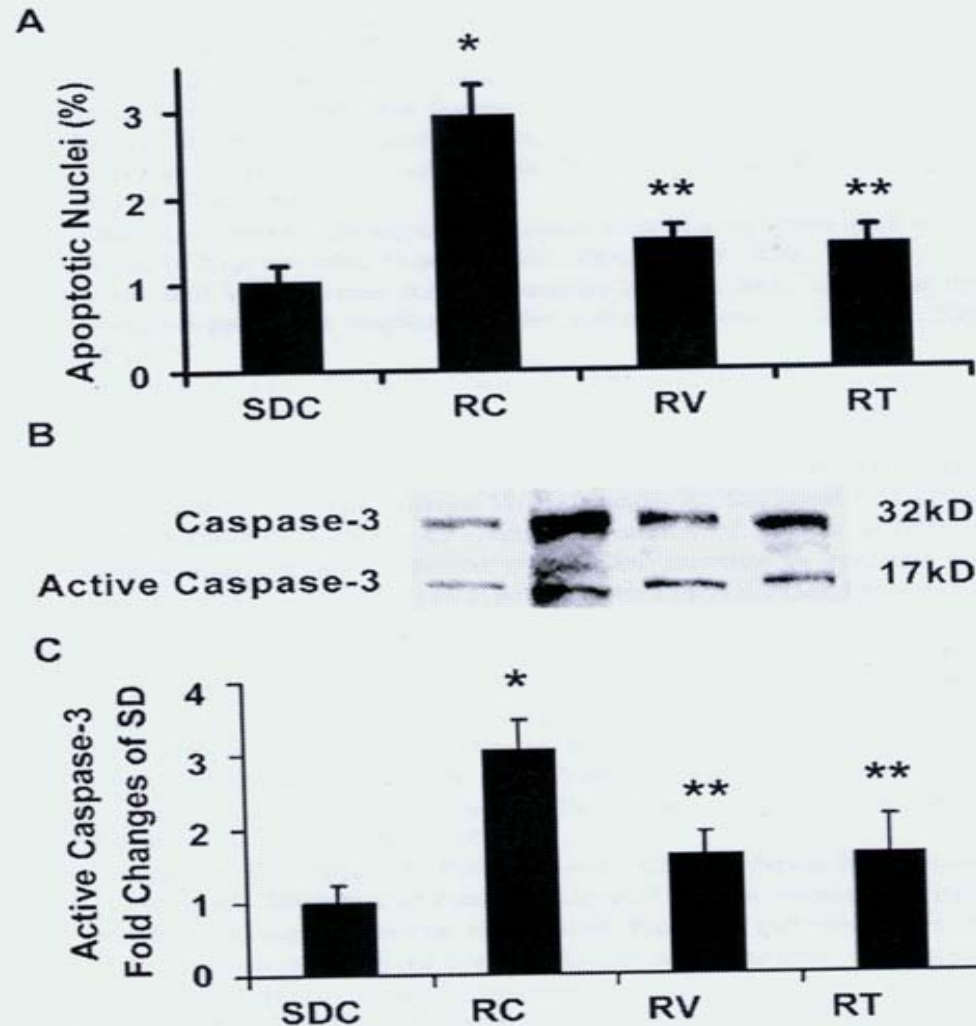
**Wall/Lumen ratio** of retinal arterioles in patients with **cerebrovascular event**  
Harazny JM, Hypertension 2007



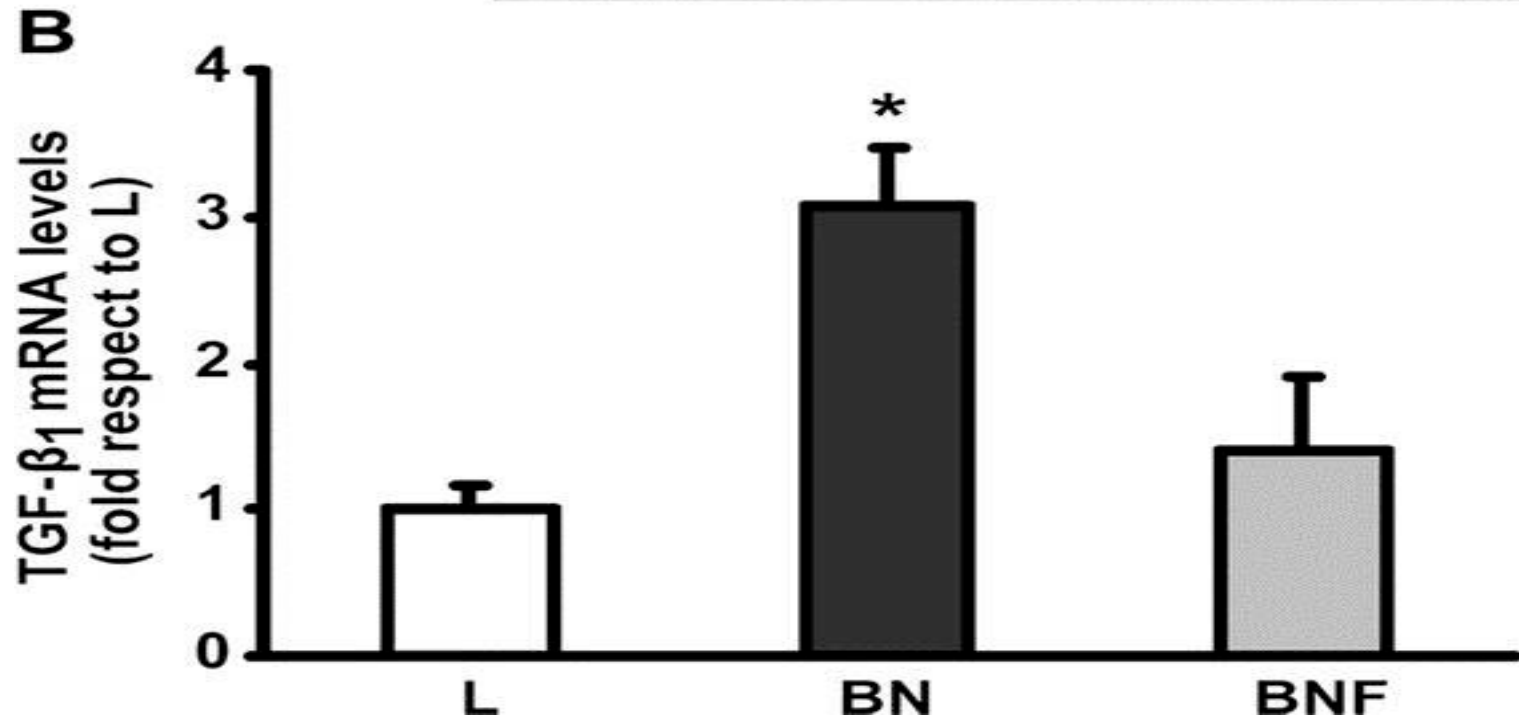
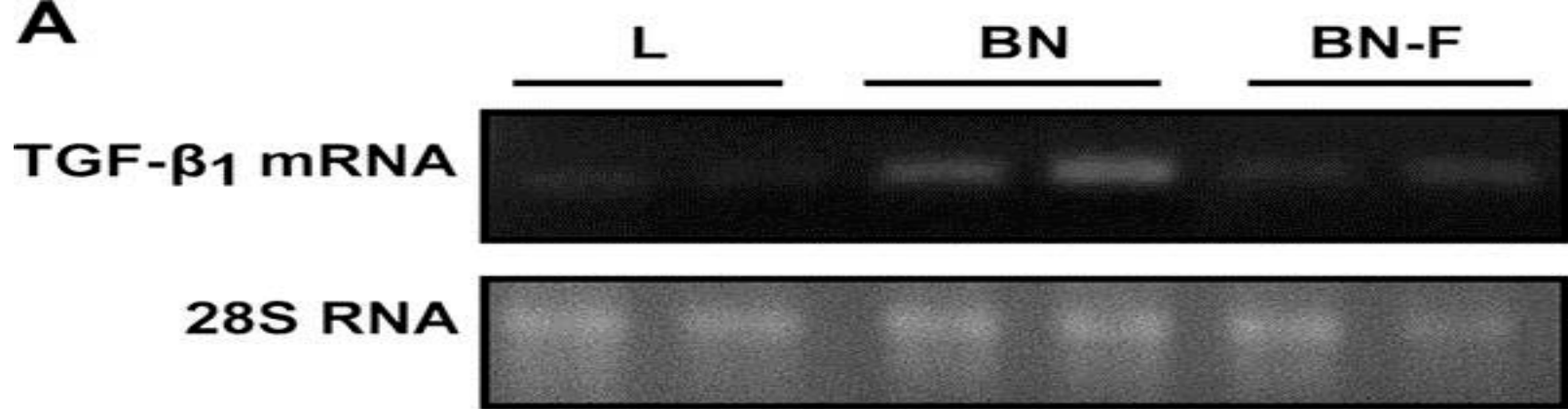
**Wall/Lumen ratio**, Harazny JM et al, Hypertension 2007



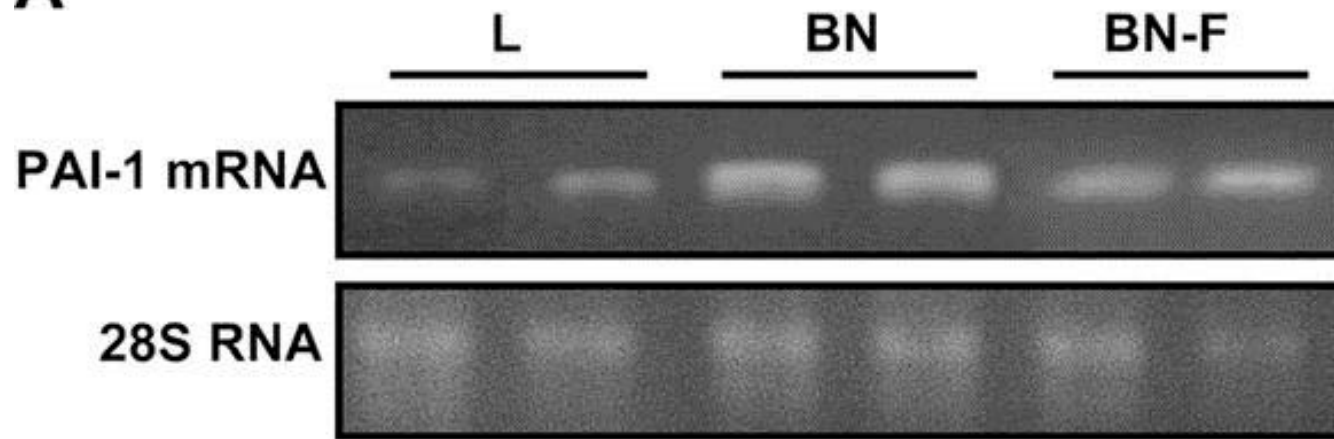
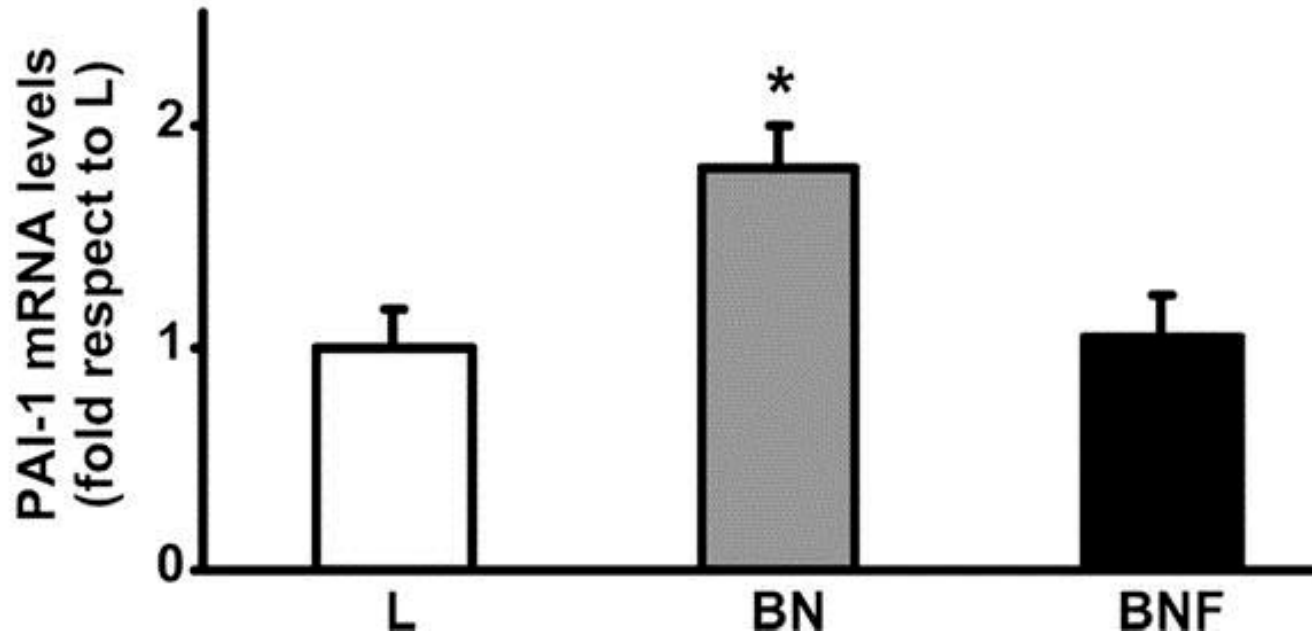
Wei et al, NADPH ox, vasc inflamm in mRen2 rat



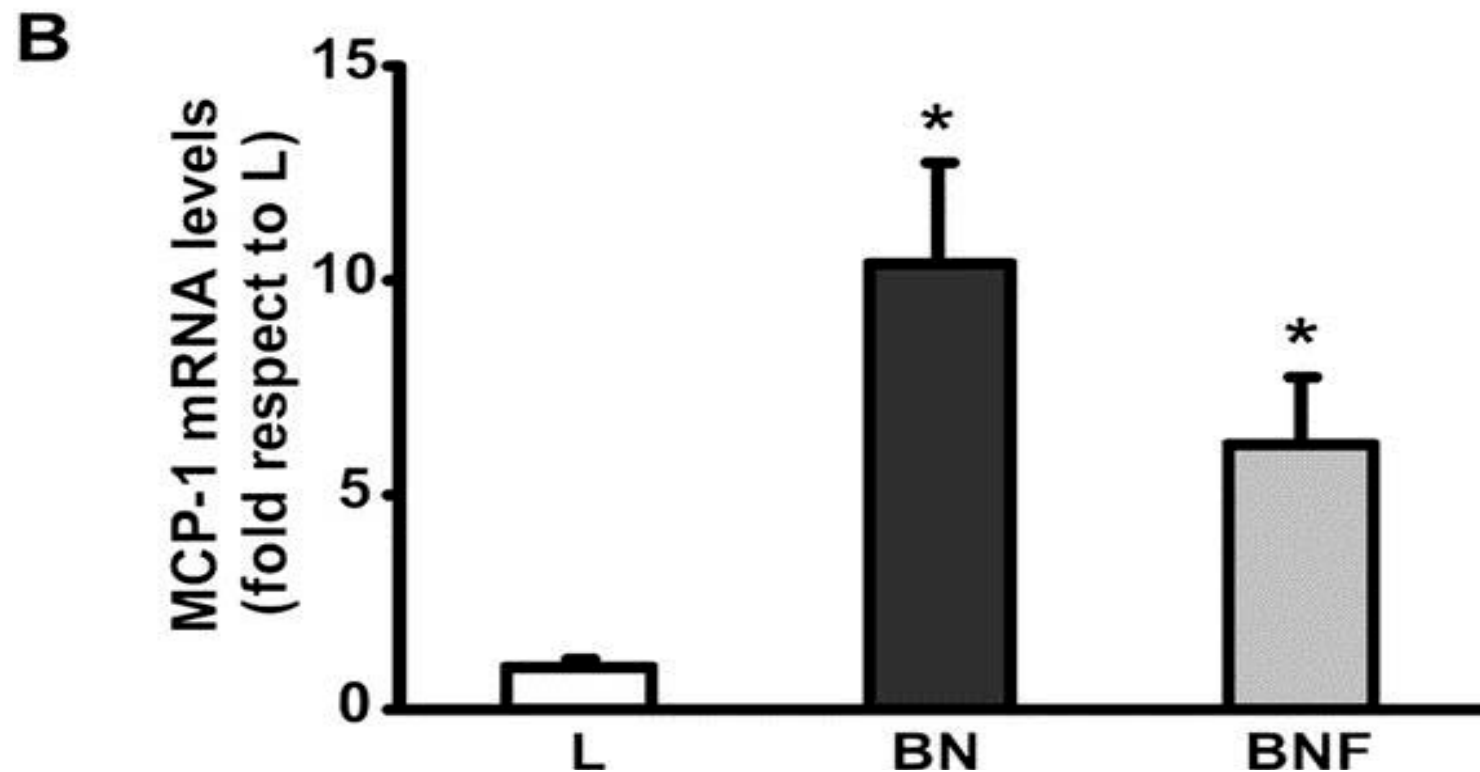
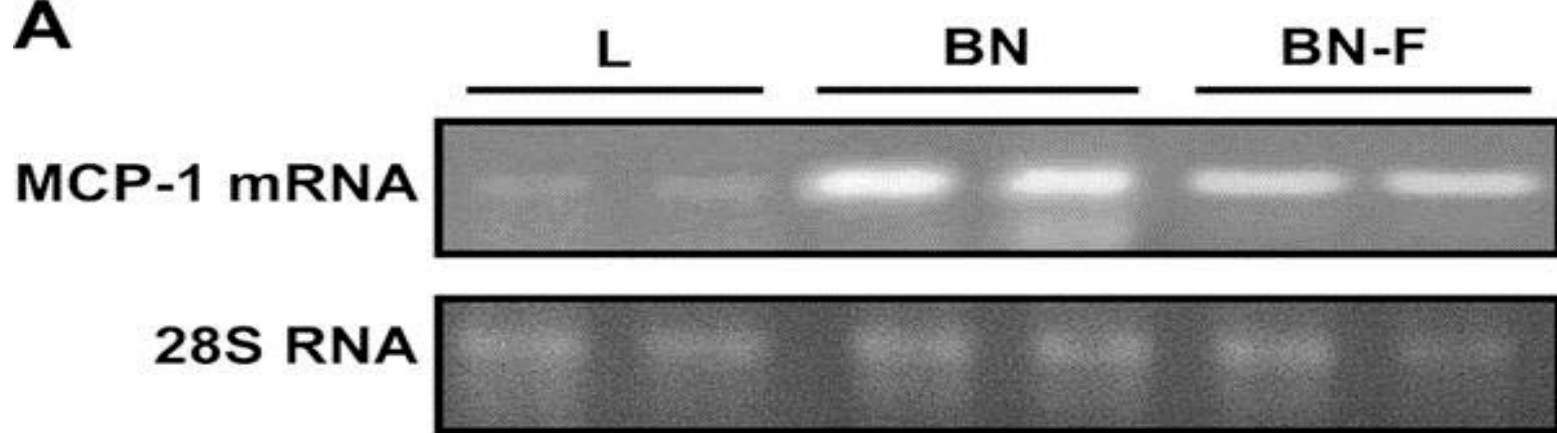
**Figure 6.** A, Apoptotic cell death as determined by TUNEL staining. TUNEL-positive and -negative cells were counted at 5 random fields. Results are expressed as number of TUNEL-positive cell/total cells  $\times 1000\%$ . B, Procaspase-3 (32 kDa) and activated caspase-3 (17 kDa) were analyzed by immunoblot, and the graph indicates quantitative densitometry analysis for active caspase-3. \* $P < 0.05$  vs SDC, \*\* $P < 0.05$  vs RC.



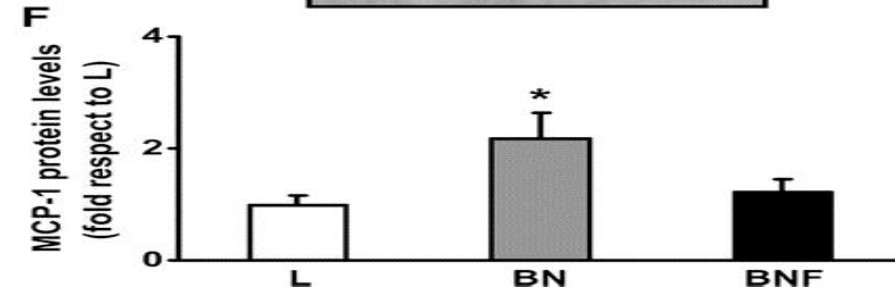
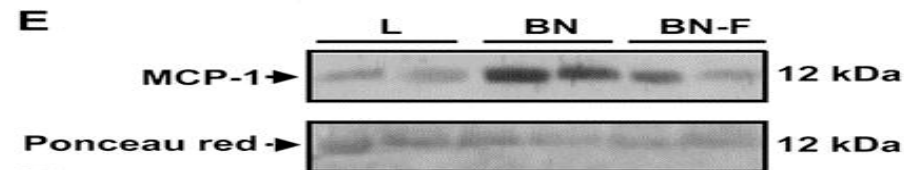
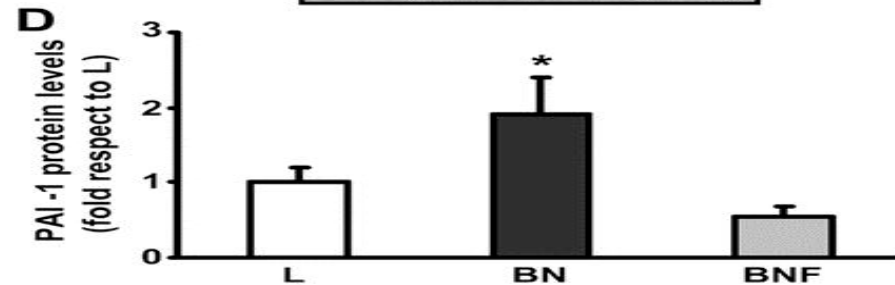
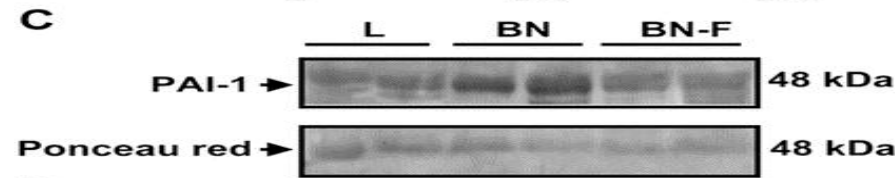
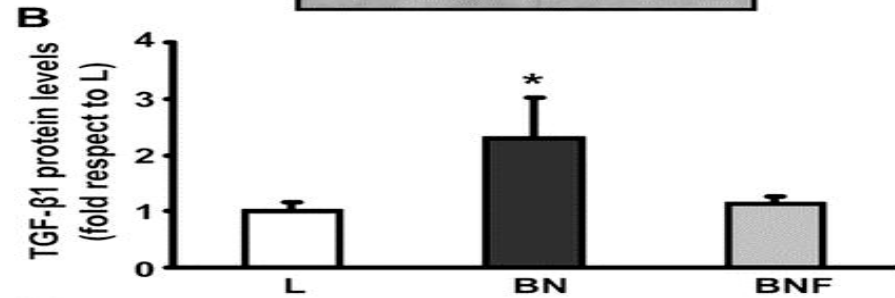
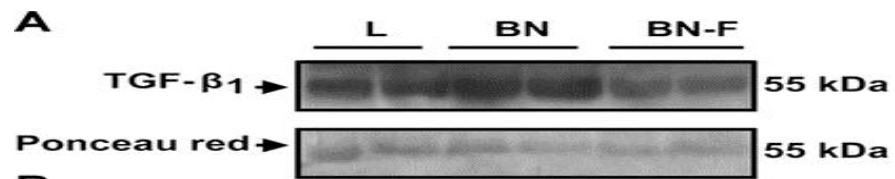
**Rho Kinase** activation and **Vascular Remodeling** in normotensive rats with high (Brown Norway) and low (Lewis) **ACE** levels  
 Rivera P et al, Hypertension 2007

**A****B**

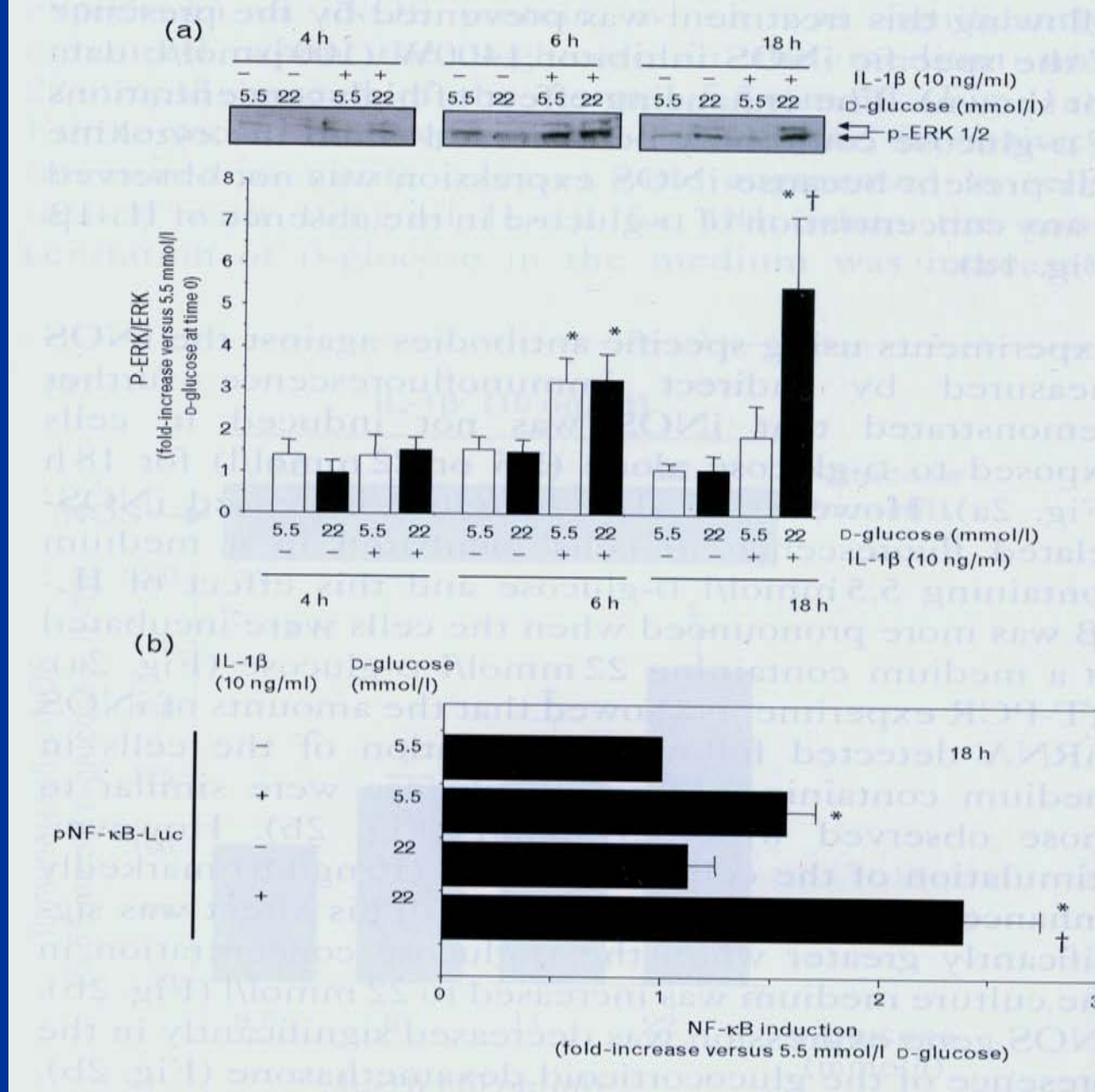
**RhoK activation-ACE-AII—inhibition by Fasudil**  
Rivera P et al, Hypertension 2007



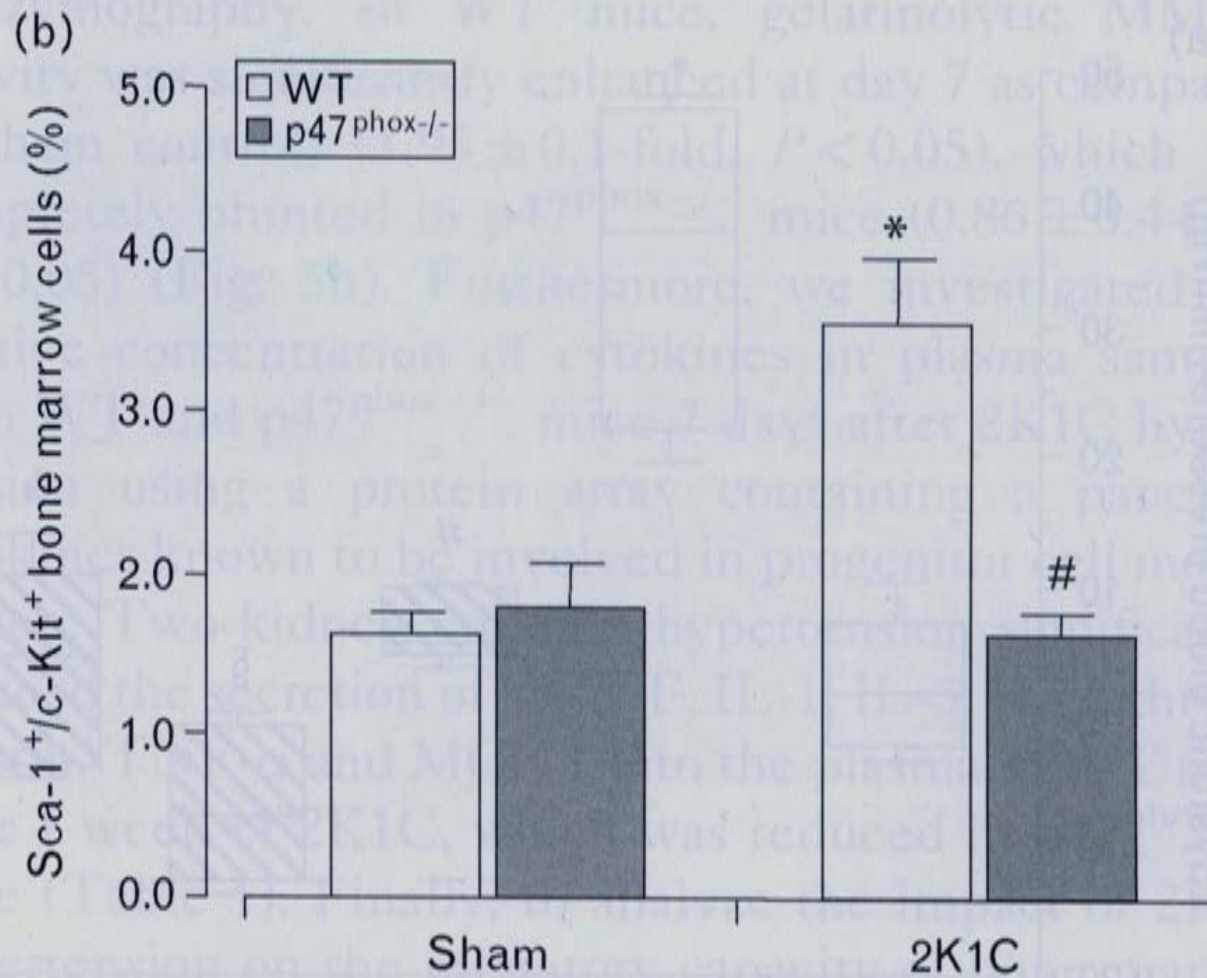




RhoK act-inhib  
Rivera et al  
Hypert 2007



Lafuente et al, J Hypert 2008 D-glucose and IL-1b in Human aortic SMC



EPC Mobilization in Renovascular Hypertension  
Salguero et al, J Hypert 2008

# Small artery remodeling in Hypertension

Effects of RAAS blockers, Ca-antagonists and  $\beta$ -Blockers

